NTNU – Trondheim
Norwegian University of
Science and Technology

Surge and Swab Pressure Calculation

Calculation of Surge and Swab Pressure
Changes in Laminar and Turbulent Flow
While Circulating Mud and Pumping

Andreas Grav Karlsen

Petroleum Geoscience and Engineering
Submission date: May 2014
Supervisor: Pål Skalle, IPT

Norwegian University of Science and Technology
Department of Petroleum Engineering and Applied Geophysics

Sammendrag

Verdens energibehov er raskt økende, og avhengigheten av olje- og gass sektoren blir stadig større for å møte dette behovet. Dette fører til en stadig økende petroleumsaktivitet rundt om i verden. Det har blitt sagt at alle de enkle brønnene har blitt boret, og at vi kun at utfordrende brønner igjen. Industrien møter samtidig økonomiske hindre, og «nedetid» er et av de mest kostbare. [Schubert, Jan 2010] Problemer kan være smale pore/oppsprekking- trykk, borehulls stabilitet, tømte formasjoner, og formasjonsskade.

Trykkendinger som resultat av Surge og Swab har i mange år blitt sett på med stor bekymring innen olje og gass industrien. Dersom trykkendringene blir for store kan det resultere i at formasjonen sprekker opp og innstrømning av formasjonsvæske i brønnen. Dette kan lede til kick, som i verste fall ender opp i en utblåsning. En utblåsning er det verst tenkelige scenariet, da dette kan lede til store økonomiske tap og sette menneskeliv i fare.

Denne oppgaven fokuserer på bakgrunns teori og utvikling av et program for å kalkulere trykkendringer i både laminær og turbulent strømning i «non-newtonian» fluider. Programmet lar deg velge hvilke sesjoner av brønnen som er ønskelige å studere, samt utregninger av ECD.

Oppgaven vil vise en utledning for en laminær modell, samt en turbulent modell som program et basert på. Den laminære modellen er videreutviklet fra Brooks modell fra 1982, og den turbulente modellen er hentet fra en utgivelse fra blant annet Saasen (2012). Programmet er testet opp mot en sensitivitetsanalyse for å få en mer grundig indikasjon på hvilke parametere som er viktigst. Programmet er dessverre ikke testet opp mot boredata da dette ikke har vært tilgjengelig.

Resultatene presentert i denne oppgaven er realistiske og gir en god indikasjon på hvilke trykkendringer som kan forventes. Programmet er brukervennlig og lett å håndtere. Det er viktig å håndtere de forskjellige parameterne som påvirker trykkedringene. Hastigheten under heise- eller senke operasjoner er viktige å kontrollere siden trykkendringene endres raskt som resultat av endret hastighet. Ved høy hastighet vil trykkendringene stige raskt. Brønnhullsgeometri er og en viktig faktor. Med et økt areal for strømningen synker trykk endringene.

Det er observert at den laminære strømningen avhenger av blant annet «Flow behavior» indeksen n og «Power Law» konstanten K. Analysen i denne oppgaven viser at dersom «Flow behavior»

indeksen synker under en verdi på 0,5 stiger trykket raskt. Trykker øker med synkende «Power Law» konstant K.

For turbulent strømning observeres det at trykket stiger eksponentielt med økende hastighet. Dette understreker viktigheten av å utføre heise- og senkeoperasjoner med riktig hastighet. Lengden på seksjonen gir en lineær endring av trykket.

For fremtidig arbeid vil det være av stor relevans å få testet modellen mot mer boredata fra industrien. Det har vært krevende å få tilgang på boredata for å teste modellen tilstrekkelig, da flere selskaper hemmeligholder sine bore rapporter.

Abstract

Pressure changes due to Surge and Swabs has in many years been a big concern in the industry. If the pressure changes become too high, the formation can fracture, and formation influx can lead to a kick. In worst case scenarios this kick can lead on to blow out and put human life in danger.

This thesis focuses the fundamental theory and on a program that can calculate the pressure changes in turbulent and laminar flow conditions for non-Newtonian fluids. The program lets you choose what sections of the well you are interested in, as well as calculations regarding ECD.

In this master thesis a program calculating Surge and Swab pressures in laminar and turbulent flow has been developed. The laminar pressures are calculated from an equation that is developed based on Brooks(1980), and the turbulent flow equation is based on the work of Saasen (2012).

The results in this thesis are based a sensitivity analysis of the laminar- and turbulent flow equation derived in this thesis. The results give realistic pressure changes and are a good indicator for what it to expect. Unfortunately was not real drilling data provided to compare the program with real drilling data results.

This study show that handling of the different parameters is important. The speed when running or pulling out of hole is important to control, since the pressure change increases rapidly as the velocity increases. Handling of the wellbore geometry is also an important factor to control. If the flow area increases, the pressure change gets higher.

In laminar flow the pressure change also depends on the Flow behavior index n, and the Power Law Constant K. It is observed that when the Flow behavior index drops below 0,5 the pressure change increases rapidly. Pressure change also increases with a decreasing Power Law constant K.

For the turbulent flow it is observed that the pressure increases exponentially with the velocity. This underlines the importance of managing the velocity during running- or tripping operations. Length of the section changes the pressures linearly.

For future work it is important to test the models up more towards real time drilling data from the industry. It has been a difficult task to access drilling data, since most drilling reports are confidential.

Preface

This master thesis was written in my final semester of my Petroleum Engineering Master Program at the Norwegian University of Science and Technology.

First of all I want to thank my supervisor Associate Professor Pål Skalle for making it possible for me to work on this exciting topic. Thank you for your guidance, feedback and great discussions both on my project and on my master thesis. Also a great thanks to National Oilwell Varo for providing useful data for the testing of my program.

Thanks to my father, Egil and my mother Lisbeth for the great encouragement and support during my studies her at NTNU.

To all my friends that have made my time here in Trondheim fantastic, thank you for great memories and good stories. Special thanks to my housemate and fellow student Asgeir for good discussions and always being positive.

Andreas Grav Karlsen

Trondheim, Mai 2014

Contents

List of figures:

Introduction

The world's energy needs are increasing and the petroleum industry is getting more and more important for fulfilling this need. This leads to increasing petroleum activity around the world. It has been stated by many that all the "easy" wells have been drilled and that we only have "difficult" wells left. Our industry is facing increasing costly incidences of pressure-related nonproductive time [Schubert, Jan 2010]. Problems include narrow pore- or fracture – pressure, windows, wellbore stability, depleted formations and formation damage. Saving time is more important than ever, since downtime is so costly. Problems related to surge and swab pressures can lead to a number of costly drilling problems such as lost circulations due to low formation fracture and fluid kick. An accurate model is important in planning drilling operations, because in challenging wells the pressure window is narrow.

When the drill string is run-in-hole with or without mud circulation through the drill string, an additional bottom hole pressure called "Surge Pressure" is created. If the surge pressure is too high, the problems the problems stated above may occur. Swab pressure is the reduction in pressure change in the wellbore. Knowing more about the pressure surges resulting from lowering and raising the drill sting is important to have a trouble free operation [Brooks, 1982].

Often we have wells with a very narrow mud window, which means that the difference between the pore pressure and fracture pressure is small. Narrow mud window is often located in deep water formations. One of the things we need to take in consideration here is the tripping speed. The tripping process will therefore take longer time, and be more costly. Creating a program that calculates the pressure changes will therefore be of help, so that we now at what speed the tripping process should be at.

It is important to take surge and swab pressures in to consideration when looking at wellbore stability. Accurate calculations of these pressures are important, so that it is know that the pressure in the wellbore will be within the limits. A high surge pressure can result in fracturing the well formation, hence lead to lost circulation. If lost circulation occur the hydrostatic pressure can fall, and again lead to influx of fluids in the formation. This can lead to a kick. When tripping out of the hole, swabbing can result in a decrease in pressure. This can lead to formation fluids flowing in to the wellbore and in a worst case scenario result in a blowout.

The objective of this thesis is to improve knowledge of surge and swab pressure changes and build a model that calculates these, focusing on both Bingham and Power Law fluids in laminar- and turbulent flow. A model is developed to calculate surge and swab pressure changes and the estimation of ECD. The two models are based on the work of Brooks (1982) and Saasen(2012). Since no data is available to test the models, a sensitivity analysis is also made to take a closer look at the different parameters, and how they affect the results.

2. Published knowledge on Surge and Swab

Surge and swab pressure is a well-known issue in the oil-industry. In 1934 pressure surges as a result of swabbing was detected as a potential reason for influx into the wellbore [Cannon, 1934]. Cannon discussed the problems as “a possible cause of fluid influx, and extreme cases blowouts”. In 1951 Goins linked surge pressures with lost circulation. Surge and swab pressures can cause a change in the bottom hole pressure, resulting in to high pressure [Burkhardt,1961]. This pressure change is due to running or tripping the drill string [Brooks, 1982] In 1988 Mitchell published a paper that extended some of the existing surge and swab models. He compared his results with the data that Burkhardt used in 1961. He concluded that in shallow wells, inertial forces and friction were the most important factors, and in deeper wells the compressibility was key. In 2012 a paper by Arild Saasen among others were presented. In this paper a new model have been developed, and tested up against the data Burkhardt used. Some of the consequences as a result of surge and swab can be catastrophic and these are presented later in this project.

2.1 Definitions of different parameters

Mud is the common name for drilling fluid.

The mud system in a drilling operation has many important functions. The most important functions of the mud are described in chapter 2.1.

Cleaning beneath the bit:

To maximize the drilling efficiency, the drilling fluid must utilize the hydraulic horsepower from the main mud pumps to sweep cuttings from the bottom of the hole as soon as they are dislodged and allow the cutters to continue to be in contact with the formation. If the cuttings are not removed, they will be ground into smaller particles and adversely affect drilling rate, mud properties, and project cost. [NOV Confidential, internal unpublished document]

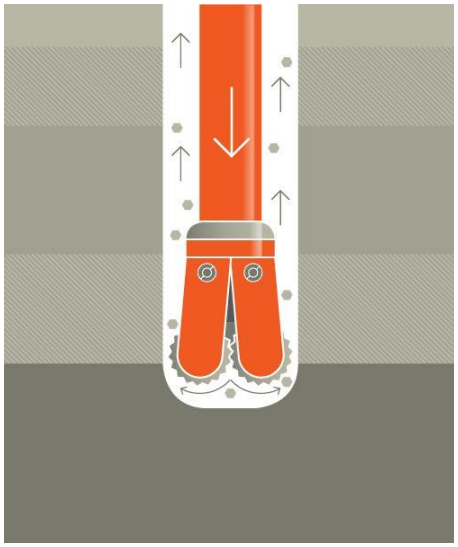

Figure 1:Cleaning beneath the bit, Survey 2014

Carrying drilled out solids from the bottom of the hole to the surface:

When the cuttings have been removed from beneath the drill bit, the fluid must transport them up towards the surface. Factors which influence movement of the cuttings are the annular velocity, the size of the cuttings, the cuttings shape, and the properties of the fluid used. [NOV Confidential, internal unpublished document]

Suspending cuttings when circulation is stopped:

Circulation of the drilling fluid is often interrupted to add additional drill pipe, change drill bits, logging and other operations. The drilling fluids must be able to suspend cuttings and weighting material while circulation is stopped, but should begin to flow easily when circulation is resumed. Properties which affect cuttings suspensions are gel strength of the mud, mud density, viscosity and the density and size of the solids in the mud. [NOV Confidential, internal unpublished document]

Allowing removal of cuttings by the surface system:

Once the mud circulates back to the surface, it is desirable to remove as much of the cuttings as possible. Most times this is accomplished with mechanical solids control equipment, such as hydrocyclones, shale shakers and centrifuges. The drilling fluid should be formulated to maximize the efficiency of the removal equipment, and then return to the tank. [NOV Confidential, internal unpublished document]

Controlling formation pressure:

The mud column in the wellbore must provide enough hydrostatic pressure to balance formation pressures and avoid collapse. The hydrostatic pressure is the pressure while the fluid is not being circulated, at any point in the wellbore depends on the depth and the density of the drilling mud. The formula used to the hydrostatic pressure is:

$$P = \rho * \text{g} * \text{h} \quad (1)$$

Where P is the pressure, rho is the density in kg/m3, g is the gravity and h is the vertical depth.

We also have to consider the circulation of the drilling fluid affects the pressure in the wellbore. The flow of fluid through the annulus exerts additional pressure. The total pressure at any point in the wellbore is the sum of the hydrostatic pressure and the pressure required to maintain circulation at that point. The total pressure is often expressed as ECD, the Equivalent Circulating pressure Density. This is the drilling fluid that would be required to produce the same pressure under static conditions. [NOV Confidential, internal unpublished document]

ECD is calculated by the following equation:

$$ECD = \rho_{mud} + \frac{\Delta p_{annular\ friction} + \Delta p_{cuttings} + \Delta p_{surge\ and\ swab} + \Delta p_{rotation} + \Delta p_{acceletraion}}{gz} \quad (2)$$

[Skalle, 2012]

ECD and Surge and Swab pressures during tripping and running are very sensitive to the fluid properties of the drilling fluid. As viscosity increases, ECD and Surge and Swab pressures increase. Increases in viscosity are caused by chemical imbalances or solid control problems; either an increase in solid content, or an increase in the concentration of colloidal particles. Also, with higher viscosities increases frictional pressure loss within the drill string, reducing the hydraulic horsepower available at the bit. [NOV Confidential, internal unpublished document] [Skalle,2012]

Promoting borehole stability:

After drilling a well in a formation the balance between the in-situ stresses and the rock strength is disturbed, also the equilibrium between sediments and the pore fluid. Figure 2 shows a simple overview of the pressures working on a wellbore. Wellbore instability often occurs in shale sections. [Skalle,2012]

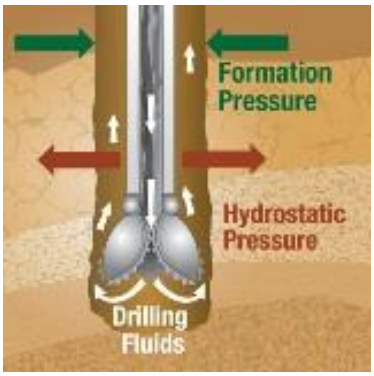

Figure 2: Pressure Overview, Survey

Many formations become unstable when exposed to freshwater based fluids. Inhibitive fluids such as those based on saltwater, natural or synthetic oils, or those containing polymers, are often required to drill them. Figure 3 shows a what can happen to a wellbore.

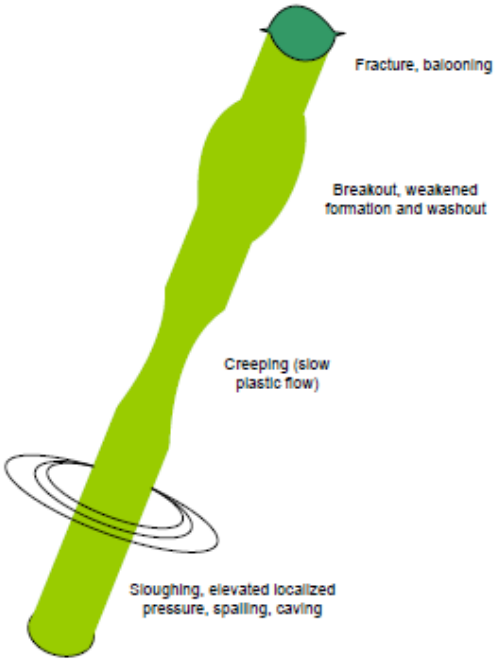

Figure 3: Wellbore instabilities,Skalle, 2012

Cooling the drill bit and lubrication the drill string:

Downhole temperatures can exceed 200 degrees centigrade. The contact of the bit with the bottom of the hole and the rotating drill string with the hole and casing generate additional heat. The drilling fluid lubricates and cools the points of contact, extending the life of the bit and the drill string. [NOV Confidential, internal unpublished document]

Helping supporting the drill string:

The fluid in the wellbore exerts a buoyant force on the drill string, reducing the effective weight that must be suspended from the derrick and handled by the hoisting system. [NOV Confidential, internal unpublished document]

Allowing accurate information to be obtained for the well:

The drilling fluid must permit electronic logging and not interfere with the analysis of drilled samples. This helps to control the well, and decreases the possibilities of well problems[NOV Confidential, internal unpublished document]

Minimizing environmental impact:

The focus on environmental damage has increased rapidly over the last couple of year. Therefore it is very important that this is taken into consideration when treating the mud. Both the fluid itself and

the cuttings generated from the well must be dealt with when drilling is completed. The cuttings may be contaminated with oil or other chemicals and have to be treated before they can be disposed of. The base fluid may also be considered a pollutant. Some disposal alternatives are; recycling for future use, cuttings – re-injections, thermal desorption and stabilization[NOV Confidential, internal unpublished document]

Relationship of Fluid Properties:

The ability of a drilling fluid to perform the way we want depends on various fluid properties. Most of these are measurable and affected by solids control.

Density is a measure of the weight of the mud in a given volume, for example kg/m^3, and often referred to as the mud weight. The instrument used to measure mud weight is the mud balance shown in figure 4. A pressurized mud balance will produce the correct mud weight even if the mud is gas cut, but most rigs use the basic mud balance. Both instruments read four different scales. Density, pressure gradient, pounds per cubic feet and specific gravity. Specific gravity is the ratio of a materials density to the density of water. Viscosity is a measure of resistance to flow and is one of the most important physical properties of drilling mud. Increasing the concentration of solids or the total surface are of the solids in a fluid, increases its velocity. [NOV Confidential, internal unpublished document]

Figure 4: Mud balance, Survey

Funnel Viscosity provide information about how mud behaves at low flow rates, such as surface pits and across shaker screens. The higher the funnel viscosity is, the thicker the fluid.

Plastic velocity measures the portion of a mud's flow resistance caused by the mechanical friction between the suspended particles and by the viscosity of the continuous liquid phase. In practical terms, plastic viscosity depends on the size, shape and concentration of solid particles in the fluid.

Yield Point is a measure of attractive forces between suspended solid particles in a liquid while it is being circulated. It measures the positive and negative attractive forces between the solid particles in a fluid. Yield point is measures with a rotating viscometer and is expressed in lbs/100ft^2. [NOV Confidential, internal unpublished document]

Filtration or Wall-Cake:

Mud liquid seeps into porous formations leaving a layer of mud solids on the exposed formation surface. This layer of mud solids is called a filter cake or some places a wall cake. The filter cake forms a barrier and reduces further filtration out to the formation. This process is referred to as filtration or fluid losses. [NOV Confidential, internal unpublished document] [Skalle,2012]

Types of drilling fluids:

Drilling fluids are generally categorized as water- and oil- or synthetic-based, in other words, weighted or unweight muds. Following is a list of typical types of mud.

1. Water-Based-Mud (WBM)
    a. Spud Mud
    b. Natural Mud
    c. Chemically-Treated Mud
        i. Lightly Treated Chemical Mud
        ii. Highly Treated Chemical Mud
        iii. Low Solids Mud
        iv. Polymer Mud (Non Dispersed Muds)
        v. Calcium Treated Mud
        vi. Silicate Treated Mud
    d. Salt Water Mud
        i. Sea Water Mud
        ii. Saturated Salt Mud
2. Oil-Based Mud (OMB) or Non Aqueous Fluids (NAFs)
    a. Diesel
    b. Mineral
    c. Synthetic-Base Mud (SBM)

i. Olefin
ii. Ester
iii. Others

Water based mud have water as the liquid phase and are used to drill most of the wells in the world because water is usually available and water based fluids are relatively simple and cheap.

Oil based mud's or Non Aqueous fluids contain diesel, mineral or synthetic oil as the continuous liquid phase and are used for wells that require maximum hole protection. NAFs are usually much more expensive than water based mud's and therefore are used only when there is a specific need. NAFs keep the hole in gauge, reducing and minimizing the risk of stuck pipe in crooked or high angle holes, where hydrate formations are being drilled. [NOV Confidential, internal unpublished document] [Skalle,2012]

2.2 Rheology

Many different types of fluids are used when drilling, this to maintain the structural integrity of the borehole, carry out cuttings and to cool the drill bit [Schlumberger Glossary, 2013]. We divide into Newtonian and non-Newtonian fluids, and in this project non-Newtonian fluids have been taken in consideration.

Drilling fluids most often behave as non-Newtonian. Non-Newtonian fluids are those in which the shear stress is not linearly related to the share rate γ. Shear rate expresses the intensity of shearing action in the pipe, or change of velocity between fluid layers across the flow path:

$$\gamma = -\frac{dv}{dr} \tag{3}$$

The fluids viscosity expresses the resistance to the fluids flow. Viscosity is due to friction between parcels of the fluid that moves with different velocity. For example honey has a higher viscosity than water. In Newtonian fluids the viscosity is at a constant level for all shear rates, shown in figure 6, and a Non-Newtonian fluid is not linearly related to the shear rate. [Skalle,2012]

Newtonian Fluids:

The viscosity of a fluid expresses its resistance to the flow. The fluids with a constant viscosity for all shear rates are called Newtonian.

It is said that a fluid is characterized as Newtonian if the viscous stresses that arise from its flow, at every point are proportional to the local strain rate and further the deformations change over time [Skalle 2012].

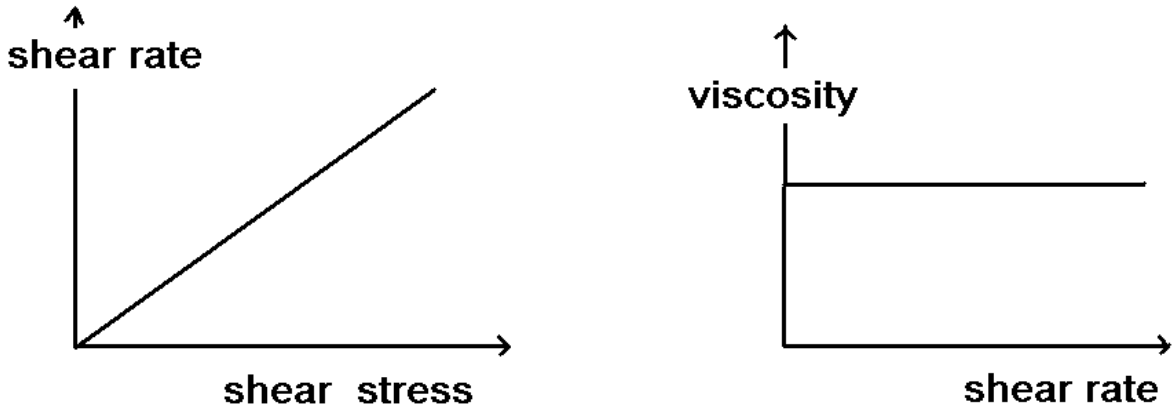

Figure 5: Description of Newtonian fluids, Survey

Power Law Fluids:

Power law fluids, also known as Ostwald-de Waele relationship is a generalized Newtonian fluid. When using a power law model, it is important to note that at very low velocities the pressure drop must exceed the pressure required to overcome gel strength, which is a function of the time the mud has remained stationary[Brooks,1981].

Bingham fluids:

A Bingham fluid is a fluid that under low shear stress acts as a rigid body and under high shear stress act as a viscous fluid. If the fluid pasts its critical shear it behaves like a Newtonian Fluid.

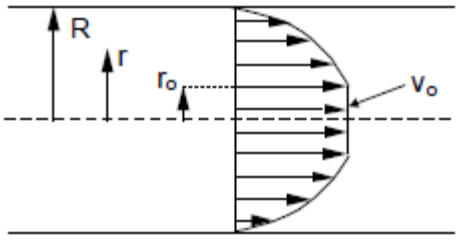

Figure 6: Flow Profile, Laminar, Bingham, Skalle 2012

Rheology of fluids:

Rheology of drilling fluids is measured and determined in the drilling industry by three different approaches.

- 2 data points oil field approach (Fann VG meter)
    - It is important to notice that due to the geometry the true shear stress, τ_w is obtained by a multiplying factor of 1.06 [Skalle, 2012]
    - The Fann VG viscometer is suited for the Bingham model.
- 2 data standard approach
- 6 data points regression approach

Lately the need for higher quality for rheology has arisen, due to an evolving industry. The Newtonian model is the simplest model. [Skalle,2012]

The most common rheological models are listed below and shown graphically in figure 7.

Newtonian model: $\tau = \mu\gamma$ (4)

Bingham plastic model: $\tau = \tau_y + \mu_{pl} * \gamma$ (5)

Power law model: $\tau = K * \gamma^n$ (6)

Herschel Bulkley model: $\tau = \tau_y + K\gamma^n$ (7)

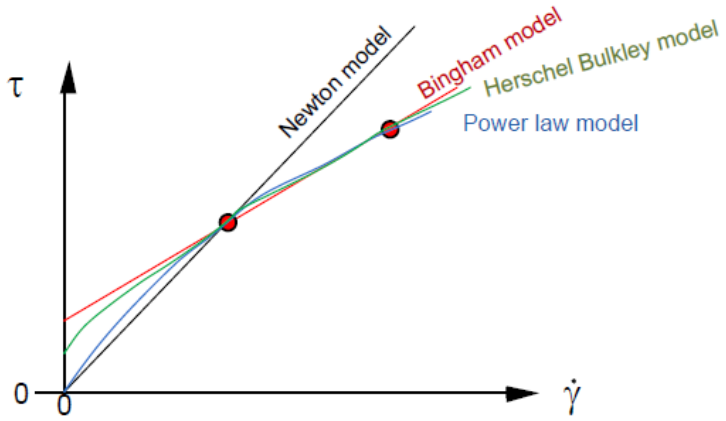

Figure 7: Rheological models, Skalle, 2012

Gel:

The gel strength is the shear stress measured at low shear rate after the drilling mud is static for a period of time. Gel strength is one of the most important properties a drilling fluid has, since it demonstrates the mud's ability to suspend drilling solids and other materiel once circulation has stopped. Another effect caused by pipe movement or pump start needs to be considered as a part of the ECD. Most mud is time dependent and tends to build up a gelled structure when quiescent. By moving the drill string axially, extra pressure is needed to break the gel that has formed on the pipe surface. The surface shear stress relates to pressure. If in a narrow zone this may lead to problems [Skalle, 2012].

$$\Delta p_{gel} = \frac{4 r_w * L}{D_{pipe}} \quad (8)$$

If the mud that is pumped is used to break the gel, the situation becomes worse. Then it must be broken first inside the drill sting and then in the annulus along two surfaces; one surface is the drill sting and the other is the wellbore.

Frictional Pressure:

A major factor contribution to surge and swab pressure in a wellbore is usually the frictional pressure drop resulting from flow of the drilling fluid. [Brooks, 1981]

Accurate knowledge of pressure surges induced by raising and lowering the drill string is of great importance in ensuring trouble free drilling operations. Procedures for calculating these pressure surges have been presented by Burkhardt, Schuh and Fontenot and Clark. The pressure loss comes from several different parts, frictional losses in annulus, acceleration of the mud column, local changes in fluid velocity and protectors.

When looking at the flow between two concentric pipes, they can be treated either as flow in true concentric pipes. It can also be looked on in a simplified manner as flow between two parallel plates. For narrow annuli the deviation between the true and parallel flow is highest, and here the losses may become a large portion of total loss, significant errors are introduced. By pressing both solutions we can pursue this difference. [Skalle 2012]

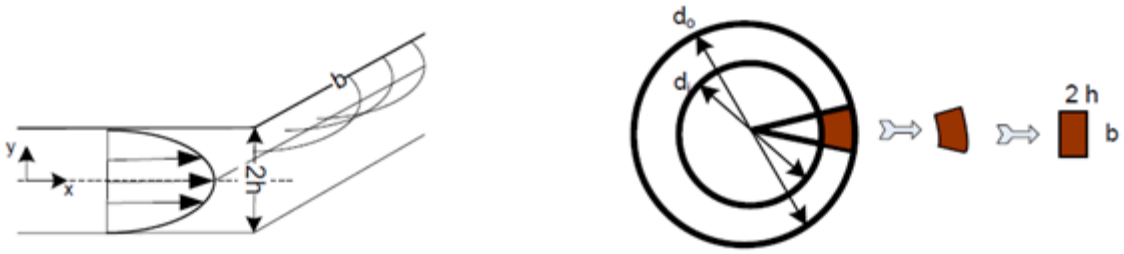

Figure 8: Geometry and velocity profile for flow between two parallel plates, Skalle 2012

Flow conditions:

We divide between laminar flow and turbulent flow, depending on the value of the dimensionless Reynolds's number, Re. When looking at flow in a straight pipe or area, the critical value between laminar and turbulent flow is a Reynolds's value of around 2300. From here on we have a transition zone, and from Re=4000 we have turbulent flow. When calculating it is divided between laminar and turbulent flow. At a Re>2300 it is calculated as a turbulent flow.

- Laminar when *Re < 2300*
- Transient when *2300 < Re < 4000*
- Turbulent when *4000 < Re*

The Reynolds's number is calculated from many different equations, depending on the area of use. The most common way of calculating the Reynolds's number is:

$$Re = \frac{\rho * v * D}{\mu} \qquad (9)$$

Where ρ is the density of the fluid, v is the velocity, D is the Diameter of the pipe / area and μ is the dynamic viscosity.

Laminar flow:

Laminar flow is a flow condition when there is no disruption between the layers. When the velocity is low, fluids tend to flow without lateral mixing, and the layers slide past one another. I laminar flow the motion of the particles of the fluid is very orderly with particles moving in straight lines, parallel to the walls of the pipe. The model used to calculate pressure change in laminar flow is derived in chapter 3.1.

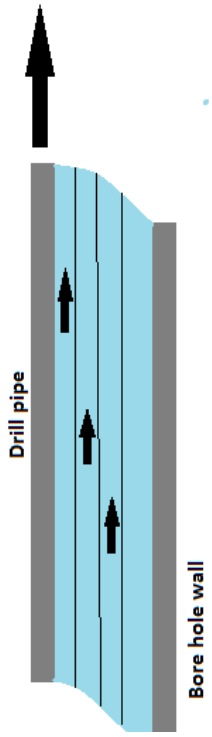

Figure 9: Laminar flow

Turbulent flow:

Turbulent flow can be described as “chaotic” property changes. eddies and wakes make the flow unpredictable. Turbulent flow happens in general at high flow rates and with larger pipes. Shear stress for turbulent flow is a function of the density - ρ. The model used to calculate the pressure change in turbulent flow is shown in chapter 3.2.

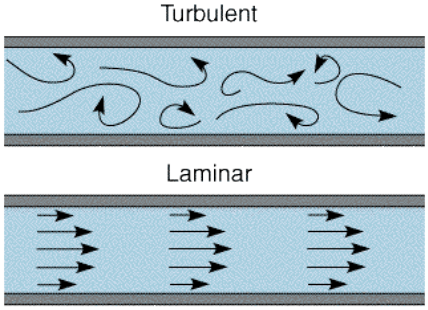

Figure 10: Turbulent vs. Laminar flow, Survey

2.3 Mud pumps

All pumps should be sized for its specific application. Choosing a suitable pump can only be done when knowledge of the system details are in place. To choose the best suited pump the following information is required:

- Fluid Temperature
- Specific gravity of fluid (the maximum)
- Pipe Diameter
- Length of pipe
- Fittings such as elbows, suction, etc.
- Elevation flow required
- Head required at end of transfer
- Type of driver required
- Power available

If the information above is not known, assumptions have to be made that can lead to pump failure, high cost due to maintenance, downtime and improper performance.

The pump speed depends on what kind of drive you want to put on the pump, from 3500 to 1150 RPM for 60Hz motors, and 3000-1000 RPM for 50Hz motors [NOV Confidential, internal unpublished document]. The total head, heron referred to as TH is the total vertical elevation, He, and the frictional head, Hf, pluss the head required at the end of the piping.

$$TH = He + Hf + head\ required\ at\ the\ end\ of\ piping \tag{10}$$

Subtract the suction head when the source of supply is above the pump.[NOV Confidential, internal unpublished document]

Figure 11 below shows where in the system the mud pumps are located, and how the system works. The pumps circulate the mud, and when it returns from the well it goes through a cleaning process before it can be circulated once more.

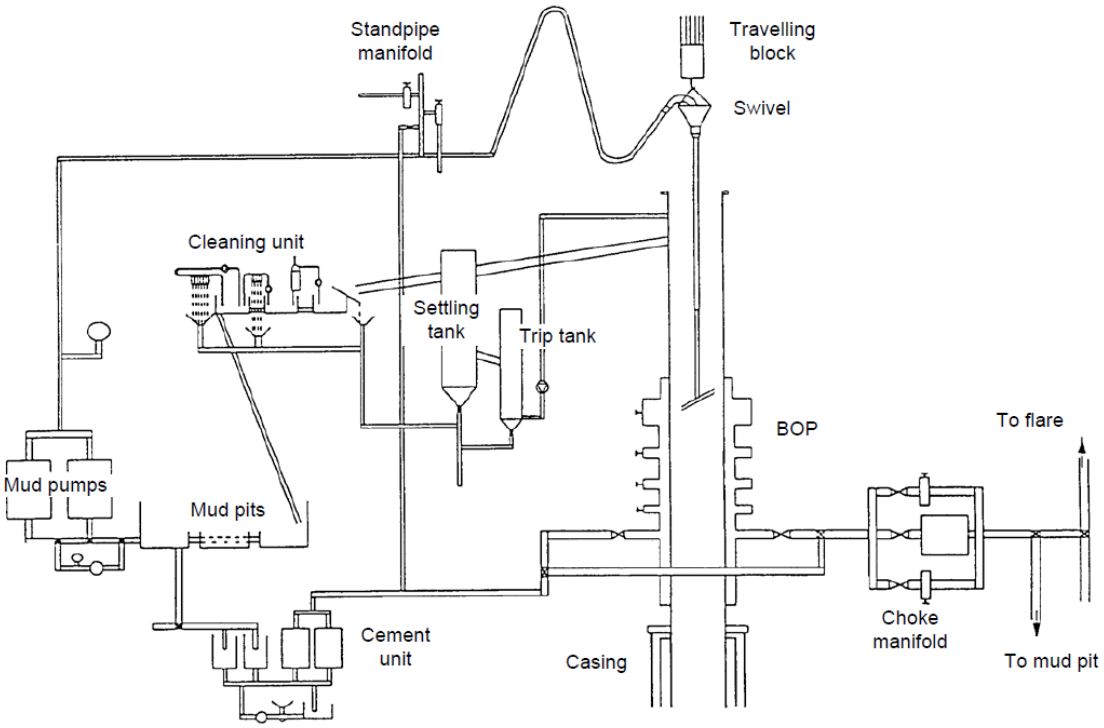

Figure 11: Mud pump in system, Skalle 2012

2.4 Problems related to Surge and Swab

Surge and swab can in worst case result in dangerous situations. If the pressure change is too big, the pressure in the wellbore can get higher than the formation fracture pressure and result in influx of formation fluids into the wellbore. This can be dangerous knowing that kicks can result in blow outs.

2.4.1 Fluid Influx

When drilling into an area where the fluid pressure is in excess of the hydrostatic pressure exerted by the drilling fluid, formation fluid will begin to displacing the fluid in the well [Naley, 2012]. When an influx for formation fluid flows into the well, we can get what is called a kick. In a worst case the well barriers fails and the influx results in a blowout.

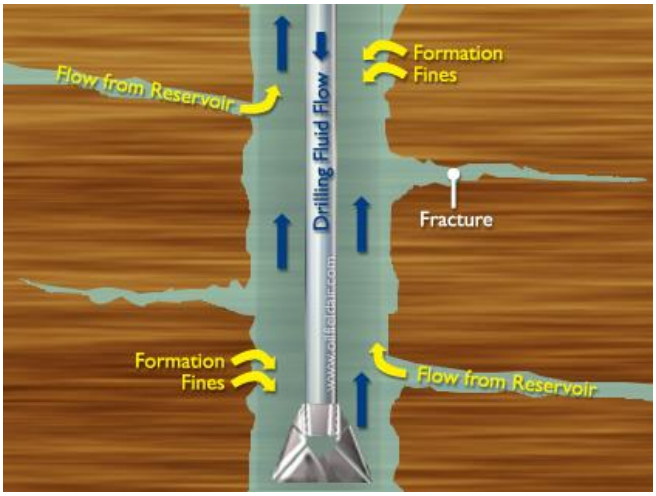

Figure 12: Formation influx, Survey

2.4.2 Lost Circulation

Lost circulation is one of the main problems related to surge pressure. Lost circulation occurs when drilling fluids flows into geological formations instead of returning through the annulus, shown in figure 12. If the margin between formation pressure and formation pore pressure is small, the surge effect can open the formation and the mud will flow out. A result from lost circulation is a reduction in the vertical height in the mud columns, which again can result other zones to flow into the wellbore.

Lost circulation can be divided into two categories:

- A minor loss - losses are between 6 and 470 barrels or 1 to 75 m^3, and remain within those amounts, or are ceased, within 48 hours.
- Severe losses - losses are greater than 470 barrels or 75 m^3, or it takes greater than 48 hours to control or cease the lost circulation.

A total loss may also happen, where the fluid are completely lost. Depending on the amount of mud lost is the category decided.

It is important to manage to control the losses, because controlled losses allow us to keep on drilling. There are many ways to control this:
Minor losses may be controlled by increasing the viscosity of the fluid with bentonite and/or polymers, or with the addition of other additives, which typically includes sawdust. The severe losses require increasing viscosity of the fluid with bentonite and/or polymers and the addition of other additives, which can be for example sawdust. [Adebayo, Chinonyere, 2012]

Total losses can be gained back by increasing the viscosity and by using additives. Other methods are for example pumping for tree branches, rags, golf balls sacks and much more, or a high viscosity fluid. If a situation where total loss occurs and the circulation cannot be regained several options are available. One can continue drilling while keeping on pumping drilling fluid, and one can continue drilling and pump sea water. This is a more used method since it is less costly. Another option is to cement the area where the loss occurred, and the continue drilling the well [Skalle, 2012].

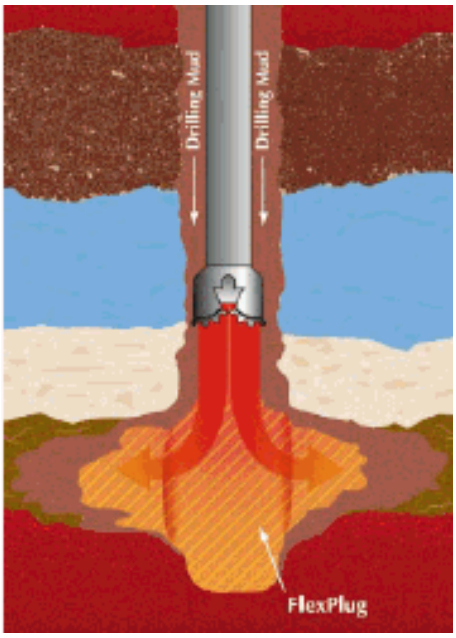

Figure 13: Loss of Circulation, Halliburton, 2013

2.4.3 Kick

The definition of a kick is flow of formation fluid or gas into the wellbore when drilling. When the wellbore pressure drops below the pore pressures, given permeable pores, fluids will enter the wellbore. If this happens the formation fluid will kick the mud out of the well and this will result in a increase in the mud pit volume. [Skalle, 2012]

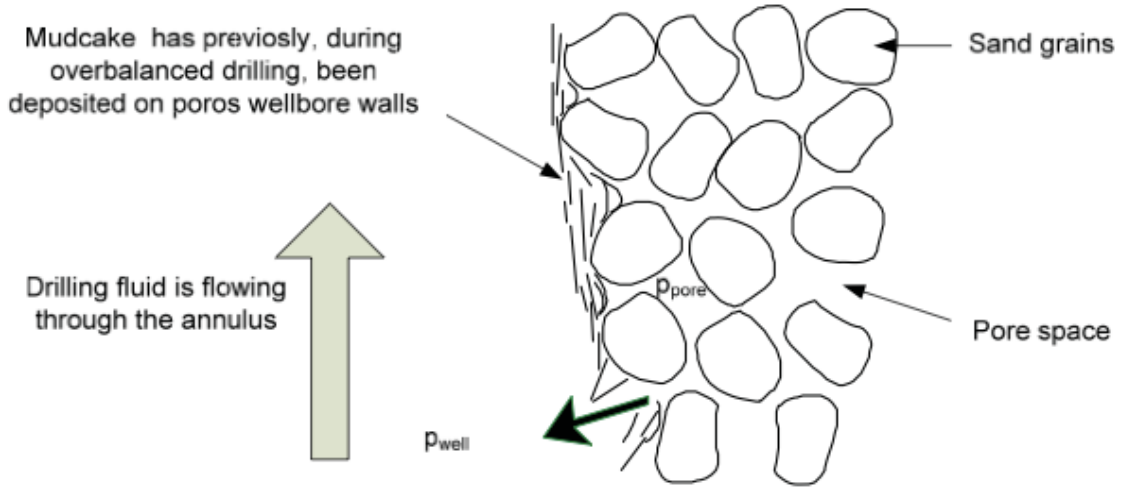

Figure 14: Kick, Skalle 2012

Kicks can be categorized in two different groups, underbalanced and induced kicks.
Underbalanced kicks are the result of drilling mud weight being insufficient of keeping the formation fluid at its place. This occurs when drilling through zones where the pore pressure is higher than expected and the mud is not adjusted to face the higher pore pressure.
Induced kicks are those who occur if dynamic or transient pressure effects lower the pressure in the well. One example of this is when pulling the drill string out of the well.
In addition to these two one may also experience kick due to hydrate dissociation. [Schlumberger glossary, 2013]
If a kick is detected it is important to take the proper action to further prevent loss of fluid and control of the well. Drillers need to be able to predict the gas behavior, because as gas flow up the wellbore it expands. This can be a great hazard for the people working on the rig, the equipment and the rig it selves.
In a case where the maximum allowed annular shut-in pressure is higher than the casing pressure, standard procedure is killing the well. To kill the well a new overbalance in the borehole must be restored. This is done by pumping mud with a higher density into the wellbore. The two main methods of doing this is today the Driller's Method and Engineer's method.
The Driller's method is a method where the formation fluid is displaced before injecting the kill mud. This is the most used method of restoring overbalance, after a kick have been detected. The Engineer's method, also called the wait & weight method is a method where the mud weight is increased and the kill mud is being pumped in immediately. [Skalle, 2012]

When dealing with a kick the proper actions are needed to be made, if not this may in a worst case lead to a blow out. A blow out is when a uncontrolled flow of reservoir fluid flow into the wellbore. Underground blowouts are the most difficult to handle. This happens when a reservoir fluid from a high pressure zone flows into a low pressure zone within the wellbore. It may take months to get these blowouts under control. A blowout can result in deaths, material damage, environmental damage and enormous economical losses.

2.4.4 Heave Motion

Today's offshore drilling is often performed by floating rigs, where heave is a major challenge. Harsh conditions as weather in the north sea and in the arctic may lead to excitation up to 13 meters. When the drill sting is suspended in the slips the drill string will follow the movement of the floater. One result from the rig heave is Surge and Swab pressures. These effects may be severe. Studies show that pulling of pipe creates swab effects of 150-300 psi (Wagner et al., 1993) and surge effects is ranging between 75-150 psi (Solvang et al,. 2008). If the pressure window is narrow in the reservoir, the surge and swab effects may be the difference between success and a catastrophe. An automatic operated choke will mitigate surge and swab effects. [NOV Confidential, internal unpublished document]

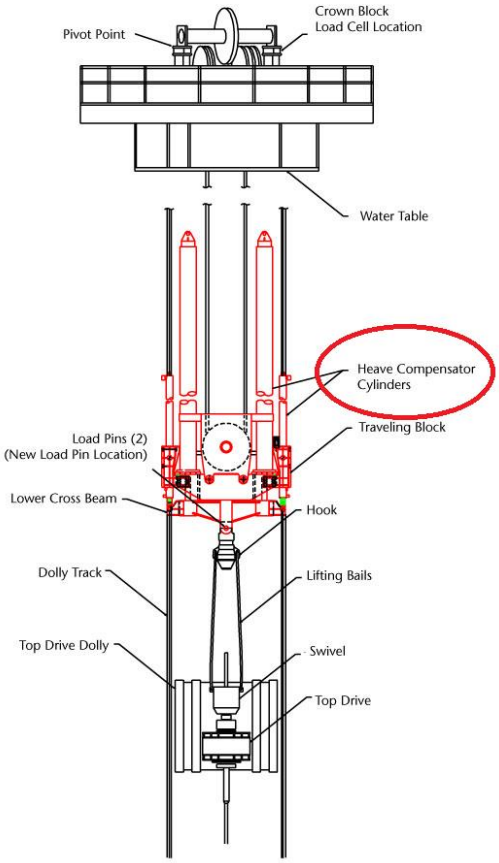

Figure 15: Heave motion system, Survey 2014

2.4.5 Equivalent Circulated Density

In cases of wells where the pore-fracture window is narrow it is a known fact that managing the Equivalent Circulated Density, heron referred to as ECD, becomes very important. In these narrow windows accurate calculations are very important not to allow influx into the wellbore. Calculations of the ECD are a result of the mud weight, rheological properties and the frictional pressure drop in the annulus due to solids loading. In addition to these, pressure change due to rotation and Surge & Swab also must be taken in consideration. It is shown previously that circulated pressure ECD related problems becomes more accurate when handling extended reach wells, ERD. In high pressure, high temperature, heron referred to as HPHT, it is show that it becomes very difficult to predict the ECD, this because the mud properties are difficult to predict. [Resort, Kinabalu 2010] Either way if not handled properly this may end up in lost circulation or another well control problem.

In the program presented in this thesis calculation of Equivalent Circulated Density is possible at any section of the well. Equation used in this calculation is taken from Pål Skalle at NTNU.

$$ECD = \rho_{mud} + \frac{\Delta p_{annular\ friction} + \Delta p_{cuttings} + \Delta p_{surge\ and\ swab} + \Delta p_{rotation} + \Delta p_{acceletraion}}{gz} \quad (2)$$

As described in the equation above you can see that many factors are to be taken in consideration. In this thesis the pressure change due to rotation and acceleration are to be neglected, since data on this have not been provided or found. In future work this should be looked at and taken into consideration. Z is the length of the section in meters. The parameters can be calculated from these equations.

2.4.6 Cling factor

The Cling factor is a factor that is little know, and very often neglected. The idea is that mud in the wellbore clings to the drill pipe and creates a “new” diameter for the drill pipe. This leads to a smaller area in the annulus, hence while tripping or running the drill string the displacement of mud has to happen in a smaller area. This leads to a high velocity and again, to a greater pressure change.

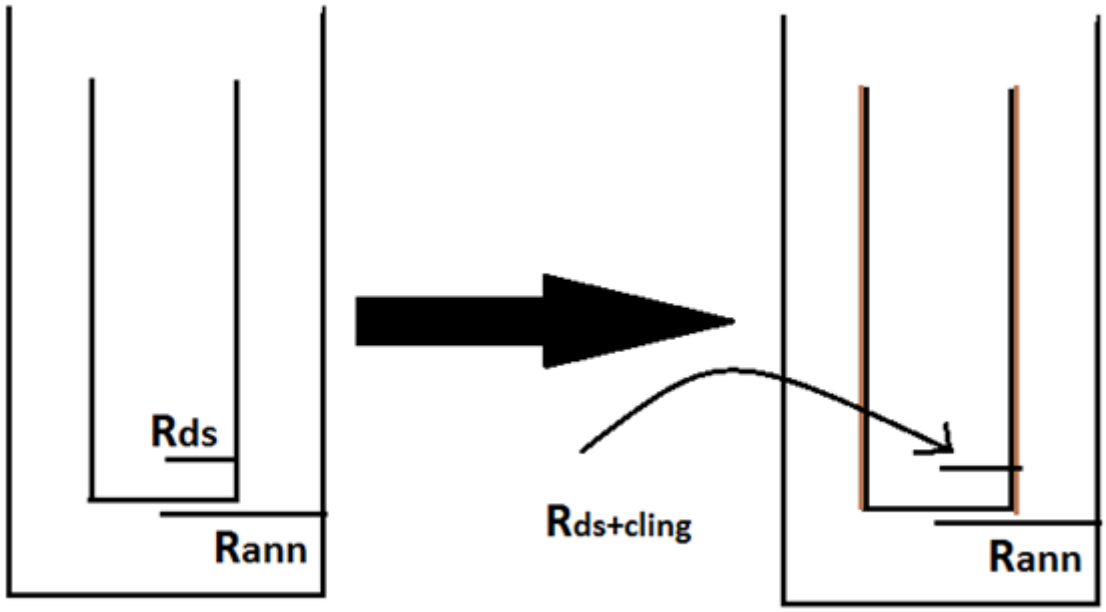

Figure 16: Cling Illustration

As illustrated in figure 16 above, you can see when the mud clings on to the drill string the area is smaller . Rann-Rds > Rann – Rds+cling.

The cling constant K_C can be expressed as following [Brooks, 1982]

$$K_C = \frac{q_{cling}}{q_{tot}} \tag{43}$$

The q_{cling} can be found by integrating from r=R_{DS} to r= $r_{ds+cling}$

r= R_{cling} and v=0

2.5 Published methods on estimating Surge and Swab

There are many methods and publications on the topic surge and swab, and they all have assumptions that make them different. The following will look at four different methods and publications.

2.5.1 Method 1 – Wellbore Pressure Surges Produced by Pipe Movement

Burkhardt (1961) was one of the first to try to make a model on surge pressures. In his paper published in 1961, he compared measured results with those predicted by his theory and showed that the magnitude of this surge could be predicted. His paper is based upon realistic assumptions, empirical equations and comparing measured surges to the ones he calculates with his model. Burkhardt's model helped calculate the surge and swab pressure for ideal Bingham plastic fluids, and applied when having a uniform wellbore, with a concentric annulus and steady state flow.

In 1974 Fontenot and Clark published and presented a paper called "An improved method for calculating surge and swab and circulated pressures in a drilling well". This was an improvement of Burckhardt's work, giving the opportunity to include Power Law fluids as well as Bingham.

2.5.2 Method 2 – Dynamic Surge/Swab Pressure Predictions

R.F. Mitchell's [1988] presents a dynamic surge and swab model that extends the existing models with the following four features. The first when pipe and annulus pressures are coupled through the pipe elasticity, and secondly longitudinal pipe elasticity and fluid viscous forces determine pipe displacement. Thirdly, fluid properties change as a function of temperature and fourth formation, pipe and cement elasticity [Mitchell 1988]. Mitchell compared his model and field data to demonstrate his results. To simulate his model he used the data from Burkhardt and Clark and Fontenot. He concludes that in shallow wells, inertial forces and friction forces seems to be most important. Steady flow surge predictions match the peak field pressures well. In deeper wells Mitchell states that compressibility is important. Steady flow surge models over predict peak pressures, and the error increases along with the depth. Negative surge pressures are less that in shallow wells.

2.5.3 Method 3 – A Medium-Order Flow Model for Dynamic Pressure Surges in Tripping Operations

The third publication I have looked at is "A Medium-Order Flow Model for Dynamic Pressure Surges in Tripping Operations". The paper was published in 2013 by Kristian Gjerstad from Teknova, Rune W. Time from UiS and Knut S. Bjørkevoll from SINTEF.

Their model is based ordinary differential equations that predict the surge and swab pressures while tripping. The model is designed for applications in real-time operations where it is important to control the pressures. The study is based on a Herschel-Bulkley non-Newtonian fluid. Their model can automatically adapt uncertain parameters or be calibrated manually. They use simplified flow equations for the laminar flow regime in drill string and annulus. In the model they chose pressure variables, P, and the volumetric flow rates Q to be the state variables. Inputs are the string velocity v, and the inlet pressure P, at the top of the drill string. For normal operations when tripping the only output is the annular pressure by the bottom hole assembly, and when circulating the flow rate into the drill string and out of annulus are looked on as outputs.

The annulus between the drill string and the wall of the borehole is divided into n segments. Each annular segment, j, in the drilling fluid is set to have a uniform pressure, Pj and a volumetric flow rate, Q. The segments have diameter D_j and inclination I_j. The Bottom hole assembly, or BHA, will always be the lowest segment, this since it is important to catch the dynamics and friction loss by the BHA and drill collars.

Conservation of mass in control volume for a compressible fluid is given as:

$$\frac{d}{dt}(\rho V) = \rho_{in} * Q_{in} - \rho_{out} * Q_{out} \tag{11}$$

Assumptions, the density are a linear function of pressure, and temperature is neglected.

$$\frac{d}{dt}(P) = \frac{K}{\rho V}(\rho_{in} * Q_{in} - \rho_{out} * Q_{out} - \rho \frac{d}{dt}(V)) \tag{12}$$

Further they assume that the density is equal in all control volumes.

$$\frac{d}{dt}(P) = \frac{K}{V}(Q_{in} - Q_{out} - \frac{d}{dt}(V)) \tag{13}$$

2.5.4 Method 4 – Surge and Swab Pressure Predictions for Yield-Power-Law Drilling fluids

In December 2012 Freddy Crespo, Ahmed, Enfis, Saasen, and Amani published a paper on Surge and swab pressure predictions.

The paper presents a new steady-state model that can account for fluid and formation compressibility and pipe elasticity. The paper consider Yield Power Law fluids, YPL.

The performance have been tested by the use of field and laboratory measurements. Comparison of these models predictions with the measurements showed a good agreement. In most of their cases the results gives results close to the measurements, this because of their realistic rheology model. The model is useful when dealing with slimhole, deepwater and ERD drilling applications.

The model is shown in the picture below and results compared to other models.

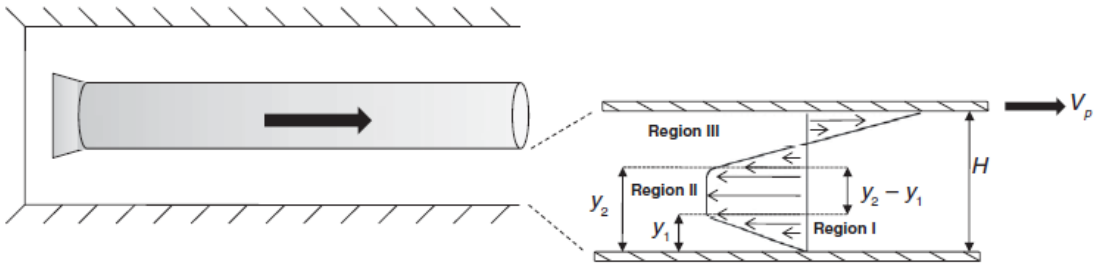

Figure 17: Overview of model

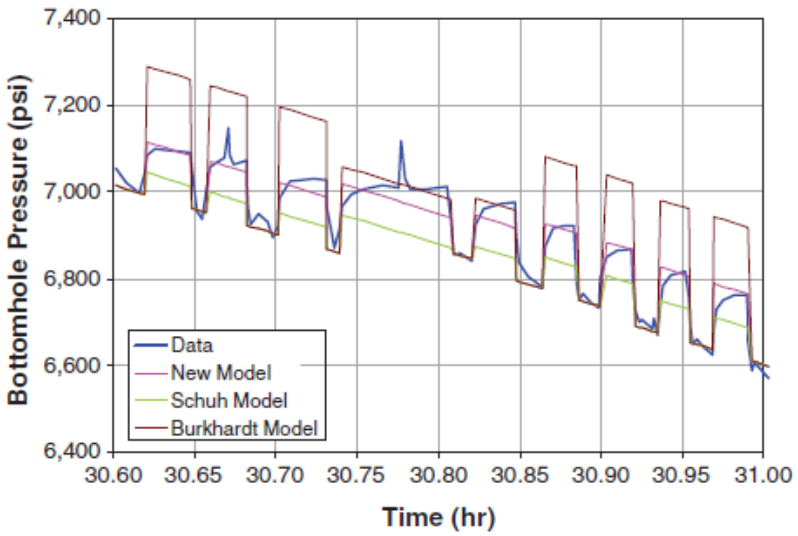

Figure 18: Compared results

3 The Selected Models

To determent the surge and swab pressure loss in laminar flow it has been worked on a model in five steps. The model is based on a paper from Brooks, A.G., Exploration Logging Inc published in 1982. In chapter 3.1, Brooks model from 1982 has been further worked on, and developed into a more user-friendly equation. This model will help develop a program to calculate the laminar pressure changes. The turbulent flow equation have been obtained from the paper by Freddy Crespo, Ahmed, Enfis, Saasen, and Amani's on Surge and swab pressure predictions from 2012. The two equations have been the base for the program developed to calculate pressure change for different wells.

3.1 –Surge and Swab – laminar pressure model

Following is the derivation of the laminar flow model.

The first step is to get an initial understanding of the surge and swab physics. It is assumed that we operate in a steady-state flow condition. The geometry is defined by the figure below.

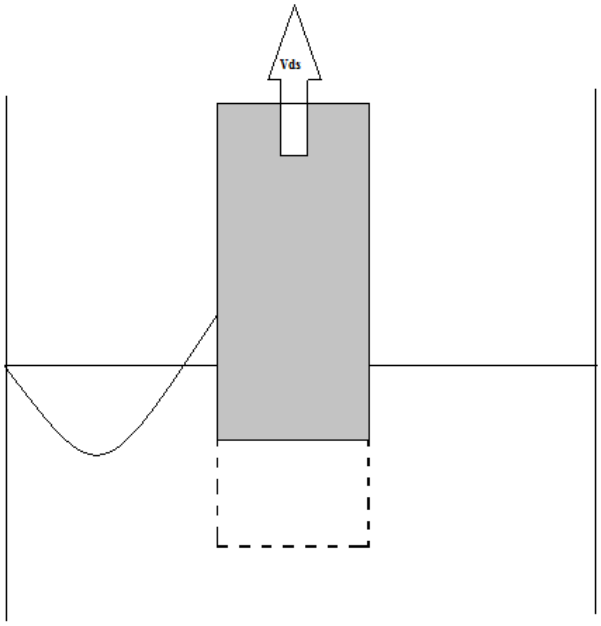

Figure 19: Geometry of wellbore

The second step is to reduce the complexity and apply simplifying assumptions. It is look at a concentric inner pipe with smooth cylinders that define annular wall and pipe wall. The assumption is that it is a closed system where pressure on the inside is the same as the pressure in the annulus. The

process is in steady state with no fluid acceleration, and Newtonian and Power law fluids are looked on.

The drill string and fluid are to be seen as elastic. Both pipe elastic and fluid viscous force are a part of determining the pipe displacement during the tripping procedure, in addition to the formation and cement elasticity. A result of this is the pressure surge.

There are three terms that are needed to determine the balancing of elastic pipe momentum. Longitudinal elasticity of pipe + pipe pressure + viscous pipe drag, showed in the equation below.

$$E * \frac{d}{dz^2} v_{pipe} + fp \frac{d}{dz} * \frac{d}{dt} * p_{pipe} + f_{drag} * \frac{d}{dt} * v \qquad (14)$$

In step 3 we look at the simplest system. A sketch is made where all the parameters are filled in like forces, radiuses and frictional constants.

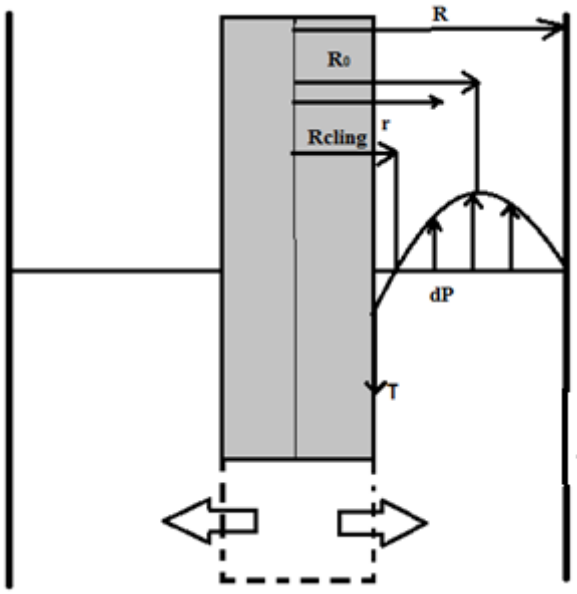

Figure 20: Geometry of wellbore with radiuses, displaced area

This drawing gives a picture of the different radiuses that are looked at. The R_{cling} is the radius of the drill string plus the amount of "clinged on" mud on the outside of the drill string. R_0 is the length from the sentrum of the drill string to the place in the annulus where the flow is at its highest, and R is the total radius in the wellbore. τ is the frictional forces from the mud on the wall and the drill string. This is where the pressure losses occur.
The forces showed in the drawing above can be expressed by the following equation [Skalle, 2012]

$$dp * A_{cross\ section} = d\tau * A_{shear} \quad (15)$$

In Step 4 an envelope is looked at with ingoing and exiting forces. To do this integrating axially needs to be done.

$$dp * \pi r^2 = \tau * 2\pi * r * dl \quad (16)$$

$$dp * r = \tau * 2dl \quad (17)$$

$$\frac{\Delta p}{2\Delta L} * r = \tau \quad (18)$$

Finally the solution can be found. When looking at a laminar flow it is usual to make an analytical solution. The problems occur when looking at more complex systems. Depending on the system one can use finite elements, other numerical methods and/or empirical solutions. In this case laminar flow is chosen. Before integrating over the envelope created in step 4, the variables needs to be differentiated.

τ = dτ , r = dr , r=R_0 , where τ= 0 to r=r.

$$\frac{\Delta p}{(2\Delta L)} * \int_{R0}^{r} dr = \int_{0}^{\tau} d\tau \quad (19)$$

$$\frac{\Delta p}{(2\Delta L)} * (r - R_0) = \tau \quad (20)$$

$$\tau = \frac{\Delta p}{(2\Delta L)} * (r - R_0) \quad (21)$$

Now the rheology model are to be included.

$$\tau = K * \gamma^n = \gamma = \left(\frac{\tau}{K}\right)^{\left(\frac{1}{n}\right)} \quad (22)$$

The shear rate in the equation above will have a positive value when $R_{DS} < r < R_0$ and a negative value when $R_0<r<R$. The shear rate is earlier in the thesis defined as: $\gamma = \frac{dv(r)}{dr}$ [1] that gives:

$$dv(r) = \left(\frac{\tau}{K}\right)^{\left(\frac{1}{n}\right)} * dr \quad (23)$$

When substituting the process shear rate and the integrate

$$\int_{Vds}^{v(r)} dv = v(r) - V_{DS} = K * \Delta p/(2\Delta L) \int_{Rds}^{r} (r - R_0)^{(\frac{1}{n})} dr \quad (24)$$

For the negative shear rate:

$$v(r) = K * \Delta p/(2\Delta L) \int_{r}^{R} (r - R_0)^{(\frac{1}{n})} dr \quad (25)$$

For r=r

$$V_{DS} = K * \frac{\Delta p}{2\Delta L} * \int_{R_{DS}}^{r} (r - R_0)^{(\frac{1}{n})} dr - K * \Delta p/(\Delta 2L) \int_{r}^{R} (r - R_{0)}^{(\frac{1}{n})} \quad (26)$$

When looking at the bulk flow it is resulting from the integral velocity across the annulus

$$q_{tot} = A * v(r)\text{dA} \quad (27)$$

dA=$2\pi dr$ and this gives

$$q_{tot} = \pi R^2 * v(r) * 2\pi r dr \quad (28)$$

When substituting and integrating, a new expression of the flow rate is obtained:

$$q_{tot} = \pi R^2 * \int_{R_{DS}}^{R} [v_{DS} + K * \Delta p/(2\Delta L) \int_{R_{DS}}^{r} ((r - R_{0)}^{(\frac{1}{n})} dr + K * \frac{\Delta p}{2\Delta L} * \int_{r}^{R} (r - R_0)^{(\frac{1}{n})} dr] * 2\pi r dr \quad (29)$$

Bulk flow rate can be expressed as:

$$q_{tot} = q_{pump} + q_{DS} = q_{tot} + A_{DS} * V_{DS} \quad (30)$$

$$\int (ax + b)^n dx = ((ax + b)^{n+1})/((n + 1)a) \quad (31)$$

Where n is gives:

n=1 → 1/n=1

n=1/2 → 1/n=2

n=1/3 → 1/n=3

Further on from here the expression above is used to express an equation for q_{tot}.

$$\int_a^b (r - R_0)^{(\frac{1}{n})} dr = \int_a^b (ar + (-R_0))^{(\frac{1}{m})}\, dr \tag{32}$$

were a =1, b=R_0 and n=$\frac{1}{m}$, and this gives (r=b in the first equation and r=a in the second equation) :

$$\frac{ax+b}{(n+1)*a} - \frac{ax+b}{(n+1)*a} \tag{33}$$

This gives:

$$[b - R_0 - \ (a - R_0) * \frac{1}{(\frac{1}{n})+1}] \tag{34}$$

Then taking a look at the two integrates within the first integral in equation [25] for q_{tot}:

$$\int_{R_{DS}}^{r} (r - R_0)^{(\frac{1}{n})} dr = \frac{1}{\frac{1}{n}+1} * [r - R_{DS}] \tag{35}$$

$$\int_{r}^{R} (r - R_0)^{(\frac{1}{n})} dr = \frac{1}{(\frac{1}{n})+1} * [R - r] \tag{36}$$

Since the two equations have the same constants in front of them I can put them together.

$$\frac{1}{(\frac{1}{n})+1} [(r - R_{DS}) + (R - r)] \tag{37}$$

$$\frac{1}{(\frac{1}{n})+1} * [R - R_{DS}]| \tag{38}$$

Further working on the equation q_{tot}. To use this equation in my MATLAB code and EXCEL program the equation is made more user friendly.

πR^2= C, $K * \Delta p/(2\Delta L)$=C1 and an expression for the two integrals within the expression is given.

$$q_{tot} = C * \int_{R_{DS}}^{R} [v_{DS} + C1 * \int_{R_{DS}}^{r} ((r - R_0)^{(\frac{1}{n})} dr + C1 * \int_{r}^{R} (r - R_0)^{(\frac{1}{n})} dr] * 2\pi r dr \tag{39}$$

Since the integral is over r, everything else can be put outside as constants.

$$q_{tot} = C * (v_{DS} * C1 * \frac{1}{(\frac{1}{n})+1} * [R - R_{DS}] * 2\pi * \int_{R_{DS}}^{R} r * dr \tag{40}$$

This gives the final expression:

$$q_{tot} = \pi^2 * R^2 * \left(v_{DS} + K * \frac{\Delta p}{2\Delta L} * \frac{1}{\left(\frac{1}{n}\right)+1} (R - R_{DS}) \right) * (R^2 - {R_{DS}}^2) \quad (41)$$

Equation [41] rearranged so the expression for Δp is:

$$\Delta p = \frac{q_{tot} * 2\Delta L}{\pi^2 * R^2 * \left(\frac{1}{\left(\frac{1}{n}\right)+1} (R - R_{DS}) \right) * \left(R^2 - {R_{DS}}^2\right) * K} - \frac{v_{DS} * 2\Delta L}{\left(\frac{1}{\left(\frac{1}{n}\right)+1} (R - R_{DS}) \right) * \left(R^2 - {R_{DS}}^2\right) * K} \quad (42)$$

Equivalent Clinging Constant:

The pressure drop is depending on the pipe velocity, thus the clinging constant can be written as:

$$K_C = \frac{q_{cling}}{q_{tot}} \quad (43)$$

The q_{cling} can be found by integrating from r=R_{DS} to r= r_{cling}

r= R_{cling} and v=0

3.2 Surge and swab – turbulent pressure calculations

The flow is often in a turbulent condition. When the Reynolds number exceeds 2300 we say that the flow hits turbulent. In turbulent flows the fluids can be described as having chaotic property change; hence other factors will be more critical for calculating the pressure change.

The model used in this thesis to calculate the pressure changes are taken from the paper that in December 2012 Freddy Crespo, Ahmed, Enfis, Saasen, and Amani published on Surge and swab pressure predictions. This equation has been chosen since it earlier has proven to give good results for turbulent flow conditions.

$$\Delta P_s = 2f * \frac{\rho(u_p+V_p)^2}{g_c * d_{p,i}} * L \qquad [44]$$

Here ΔP_s the pressure changes are a result from surge or swab. f, is the fanning friction factor, ρ is the density of the drilling fluid, u_p, the fluid velocity, v_p is the drill string velocity, d is the inner diameter and L is the length of the pipe.

The fanning constant can be found from the Moody diagram seen beneath. In the program created in this thesis the fanning factor will be calculated automatically, since it is a direct result of the Reynolds-number that also is calculated.

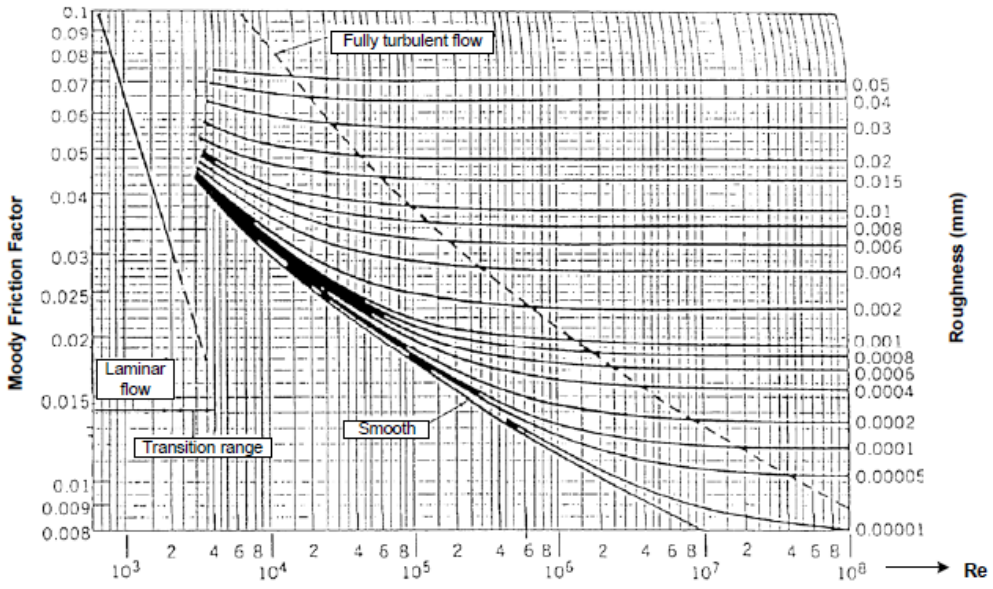

Figure 21: Moody friction vs roughness, Skalle 2012

4. Test data and sensitivity analysis

Acquiring good and relevant test data to simulate the results for this program has been challenging. Few companies are willing to shear their data, but some data has been collected. National Oilwell Varco has been helpful and provided some drilling data that were used when performing the sensitivity analysis. Since only some of the data were provided it was not possible to compare the results.

4.1 Drilling data

The quality of the drilling data received from National Oilwell Varco is of good quality and gives a good base to create an analysis around realistic values. The drilling data has therefore data been used as a basis for the analysis done. Some of the parameters needed to calculate the pressure change has not been provided, such as the Power Law Constant and the mud velocity, and have been set to normal values.[Skalle,2012] In the report the drilling company performed the following:

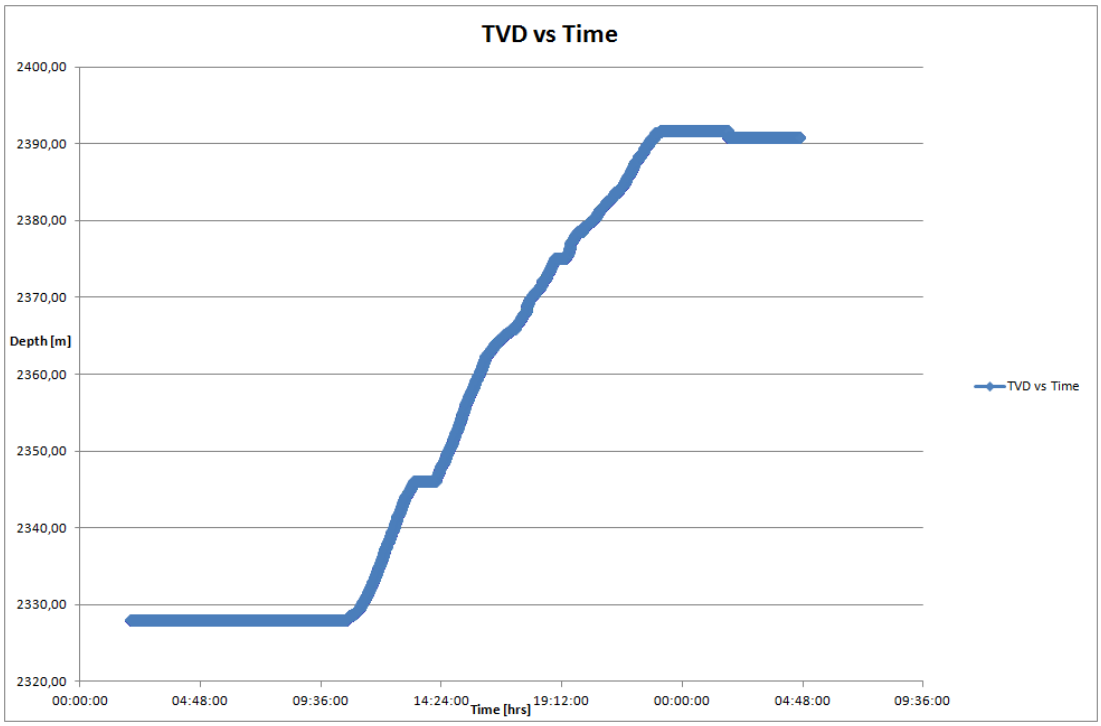

Figure 22: Daily Drilling Report, Internal unpublished document, NOV

4.2 Sensitivity analysis for laminar flow

Due to the lack of drilling data available a sensitivity analysis has been done to look at the different parameters affecting the pressure change in the wellbore. The analysis is based in the derivation from chapter 3.1. The sensitivity analysis looks closer at three different parameters, the power law constant, K, the flow behavior index, n and the velocity, v. The analysis gives a better overview of what parameters are most important to manage, in order to controlling the pressure changes. The document used to do this sensitivity analyses is attached in this master thesis.

Fixed Input

R	0,108	m
Rds	0,025	m
dL	70,000	m
Areal,A	0,02139754	m^2
Pi	3,14	

Variable input

	K (Pas)	n (-)	vds (m/s)	dP (bar)
a	0,6	1,000	0,33	
b	1,4	0,500	0,66	
c	2,2	0,333	1,00	

Figure 23: Input data laminar flow, analysis

The analysis provides 27 different cases, all the different scenarios from the values above. The method is shown in figure 24 below. The wellbore geometry is set to normal values and the bottom hole assembly has been set to 70 meters. In chapter 6 the results of the analysis are presented.

Test Matrix Set-up

Case	K	n	vds
1	a	a	a
2	a	a	b
3	a	a	c
4	a	b	a
5	a	b	b
6	a	b	c
7	a	c	a
8	a	c	b
9	a	c	c
10	b	a	a
11	b	a	b
12	b	a	c
13	b	b	a
14	b	b	b
15	b	b	c
16	b	c	a
17	b	c	b
18	b	c	c
19	c	a	a
20	c	a	b
21	c	a	c
22	c	b	a
23	c	b	b
24	c	b	c
25	c	c	a
26	c	c	b
27	c	c	c

Simulation

Sensitivity

Case	K	n	vds	Qtot	dP
1	0,6	1	0,33	0,007061	-1,37909
2	0,6	1	0,66	0,014122	-2,75818
3	0,6	1	1	0,021398	-4,17906
4	0,6	0,5	0,33	0,007061	-2,06864
5	0,6	0,5	0,66	0,014122	-4,13727
6	0,6	0,5	1	0,021398	-6,2686
7	0,6	0,333333	0,33	0,007061	-2,75818
8	0,6	0,333333	0,66	0,014122	-5,51637
9	0,6	0,333333	1	0,021398	-8,35813
10	1,4	1	0,33	0,007061	-0,59104
11	1,4	1	0,66	0,014122	-1,18208
12	1,4	1	1	0,021398	-1,79103
13	1,4	0,5	0,33	0,007061	-0,88656
14	1,4	0,5	0,66	0,014122	-1,77312
15	1,4	0,5	1	0,021398	-2,68654
16	1,4	0,333333	0,33	0,007061	-1,18208
17	1,4	0,333333	0,66	0,014122	-2,36416
18	1,4	0,333333	1	0,021398	-3,58206
19	2,2	1	0,33	0,007061	-0,37612
20	2,2	1	0,66	0,014122	-0,75223
21	2,2	1	1	0,021398	-1,13974
22	2,2	0,5	0,33	0,007061	-0,56417
23	2,2	0,5	0,66	0,014122	-1,12835
24	2,2	0,5	1	0,021398	-1,70962
25	2,2	0,333333	0,33	0,007061	-0,75223
26	2,2	0,333333	0,66	0,014122	-1,50446
27	2,2	0,333333	1	0,021398	-2,27949

Figure 24: Sensitivity analysis laminar flow calculations

4.3 Sensitivity analysis for turbulent flow

The analysis made on the turbulent flow equation is done the same way as the laminar. The analysis looked at the effects of fanning friction factor f, length of the section L, diameter d_{ds} and the velocity v. The calculations are based on the equation in chapter 3.2 and results are presented in chapter 6.

ρ	1800,000	kg/m3
dds	0,140	m
up	1,000	m/s
g	9,81	m/s^2

	f []	L (m)	v [m/s]	dP (bar)
a	0,1	50,000	1,00	
b	0,125	75,000	2,00	
c	0,15	100,000	3,00	

Figure 25: Input data turbulent flow, analysis

As seen in figure 25 and 26 the input and the parameters tested gives out 27 different cases and results.

Test Matrix Set-up

Case	K	n	vds
1	a	a	a
2	a	a	b
3	a	a	c
4	a	b	a
5	a	b	b
6	a	b	c
7	a	c	a
8	a	c	b
9	a	c	c
10	b	a	a
11	b	a	b
12	b	a	c
13	b	b	a
14	b	b	b
15	b	b	c
16	b	c	a
17	b	c	b
18	b	c	c
19	c	a	a
20	c	a	b
21	c	a	c
22	c	b	a
23	c	b	b
24	c	b	c
25	c	c	a
26	c	c	b
27	c	c	c

Simulation

Sensitivity

Case	f	L	vds	dP
1	0,1	50	0,0635	1,155818825
2	0,1	50	0,1143	0,64212157
3	0,1	50	0,1397	0,525372193
4	0,1	75	0,0635	1,733728238
5	0,1	75	0,1143	0,963182354
6	0,1	75	0,1397	0,78805829
7	0,1	100	0,0635	2,311637651
8	0,1	100	0,1143	1,284243139
9	0,1	100	0,1397	1,050744387
10	0,125	50	0,0635	1,444773532
11	0,125	50	0,1143	0,802651962
12	0,125	50	0,1397	0,656715242
13	0,125	75	0,0635	2,167160298
14	0,125	75	0,1143	1,203977943
15	0,125	75	0,1397	0,985072863
16	0,125	100	0,0635	2,889547063
17	0,125	100	0,1143	1,605303924
18	0,125	100	0,1397	1,313430483
19	0,15	50	0,0635	1,733728238
20	0,15	50	0,1143	0,963182354
21	0,15	50	0,1397	0,78805829
22	0,15	75	0,0635	2,600592357
23	0,15	75	0,1143	1,444773532
24	0,15	75	0,1397	1,182087435
25	0,15	100	0,0635	3,467456476
26	0,15	100	0,1143	1,926364709
27	0,15	100	0,1397	1,57611658

Figure 26: Sensitivity analysis turbulent flow calculations

The calculations are attached.

5. Program

The program created in this thesis is an EXCEL based program that calculates the pressure changes in the wellbore due to surge and swab. The program processes the input data to check if the flow is laminar or turbulent.

Surge				
Input data				
General information				
Diameter Drill Sting	Dds	0,1397	[m]	
Mud denisty	ρ	1200	[kg/m^3]	
Formation pressure	Pform	320	bar	
Wellbore pressure	Pwell	350	bar	
Pi		3,14		
Section 1:				
Drill Sting Diameter	Dds	0,1397	[m]	
Borehole Diameter	Dwell	0,3048	[m]	
Diamter Annulus	Dann	0,1651	[m]	
Mud Density	ρ	1200	[kg/m^3]	
Velocity drill string	v	0,4673435	[m/s]	
Dynamic Viscosity	μ	0,0042	[Pa*s]	
Length of Section	L	50	[m]	
Flow	qtot	0,01	[m^3/s]	
Area wellbore	Aw	0,0729289	[m^2]	
Area Drillstring	Ads	0,0153201	[m^2]	
Area Annulus	Aann	0,0213975	[m^2]	
Power law constant	K	1		
Flow behavior index	n	0,33		
Fanning friction factor	f	0,1023972		
Velocity fluid	up	0,1	[m/s]	
Section 2:				
Drill Sting Diameter	Dds	0,1397	[m]	

Figure 27: Input section for one of six sections

Further on, the program chooses the pressure change model based on the flow conditions. To calculate the turbulent pressure change the fanning friction factor is calculated as a result of the value of the Reynolds number. The calculations are based on the equations shown in Chapter 3. The picture underneath shows the calculations for pressure change as a result of the input data. Note that all pictures with calculations in Chapter 5 have example values, and are not linked to the actual results.

Calculations		
Reynold number, Laminar if Re<2300, Turbulent if Re>2300		
Section 1	22045,26	Turbulent
Section 2	35823,548	Turbulent
Section 3	57317,676	Turbulent
Section 4	57317,676	Turbulent
Section 5	43472,827	Turbulent
Section 6	71647,095	Turbulent

Turbulent pressure drop calulations					
Section 1	ΔP=	2885,99736	[Pa]	0,02886	[bar]
Section 2	ΔP=	159133,2001	[Pa]	1,591332	[bar]
Section 3	ΔP=	1706774,577	[Pa]	17,06775	[bar]
Section 4	ΔP=	568924,8589	[Pa]	5,689249	[bar]
Section 5	ΔP=	222666,4251	[Pa]	2,226664	[bar]
Section BHA	ΔP=	311140,079	[Pa]	3,111401	[bar]

Laminar pressure drop calculations								
Section 1	ΔP=	363,1470895	-	83,72317	279,42392	[Pa]	0,002794	[bar]
Section 2	ΔP=	17850,54045	-	1894,984	15955,5562	[Pa]	0,159556	[bar]
Section 3	ΔP=	128880,9021	-	7858,879	121022,023	[Pa]	1,21022	[bar]
Section 4	ΔP=	42960,30069	-	2619,626	40340,6745	[Pa]	0,403407	[bar]
Section 5	ΔP=	28640,20046	-	1324,578	27315,6229	[Pa]	0,273156	[bar]
Section BHA	ΔP=	16182,0329	-	1061,191	15120,8417	[Pa]	0,151208	[bar]

	Section 1	Section 2	Section 3	Section 4	Section 5	Section BHA	Total ΔP	Total ΔP
Phase:	Turbulent	Turbulent	Turbulent	Turbulent	Turbulent	Turbulent	DS	BHA
ΔP=	0,02885997	1,591332001	17,06775	5,689249	2,226664	3,11140079	26,60385	3,111401

Figure 28: Pressure change calculations

It is possible to decide what calculations the program are to do, for instance you can look at the pressure change around the bottom hole assembly. or the whole system, shown in figure 29. The positive or negative pressure change gives the new bottom hole pressure. Note that if the new bottom hole pressure is higher than the formation fracture pressure, the warning “Wellbore pressure is higher than formation fracking pressure” will appear. If the pressure is within the fracture limits nothing is shown.

Output			
Output for the calculation sheet			
Surge and Swab Pressure Change			
Pressure Loss over BHA	YES	3,1114	bar
Pressure Loss over the drill string:	YES	6,6039	bar
Total pressure change due to Surge and sw	YES / NO	9,7153	bar
New Pressure in wellbore, when pressure change is added			
Bottom hole pressure		350	bar
Total pressure change due to Surge and swab is:		29,7153	bar
New bottom hole pressure:		379,715	bar
Wellbore pressure is higher than formation pressure!!!!			

Figure 29: Functions of program

The program also calculates the ECD and the same option is possible for these calculations. The user can decide where in the wellbore the ECD value is of interest. For simplicity and due to lack of data available, the pressure change due to acceleration and rotation of drill string is neglected. However, if the data were available it should be included to get an more accurate calculation. The results in the output calculations, shown I figure 30 and 31, are calculated in a separate sheet and linked together.

ECD Calculations Section 1		
ρ_{mud}	1200	[kg/mg^3]
$\Delta p_{annular\ friction}$	0	[Pa]
$\Delta P_{cuttings}$	0	[Pa]
$\Delta P_{surge\&swab}$	2885,99736	[Pa]
$\Delta P_{rotation}$	0	[Pa]
$\Delta P_{acceleration}$	0	[Pa]
g	9,81	[m/s^2]
z	50	[m]
ECD	**1205,883787**	**[kg/mg^3]**

Figure 30: ECD Calculations

Equivalent Circulating Density			YES
Section 1	YES	1205,88	[kg/m^3]
Section 2	NO		[kg/m^3]
Section 3	NO		[kg/m^3]
Section 4	NO		[kg/m^3]
Section 5	NO		[kg/m^3]
Section 6	NO		[kg/m^3]

YES
NO

Figure 31: Choosing ECD output

The program processes the input data, calculates the value's that is wanted and shows them in the output section. Of the many sheets in the EXCEL program attached, the "Main Sheet" is the only sheet that needs to be changed. Figure 32 shows a flow chart, describing the program The program is attached in this thesis.

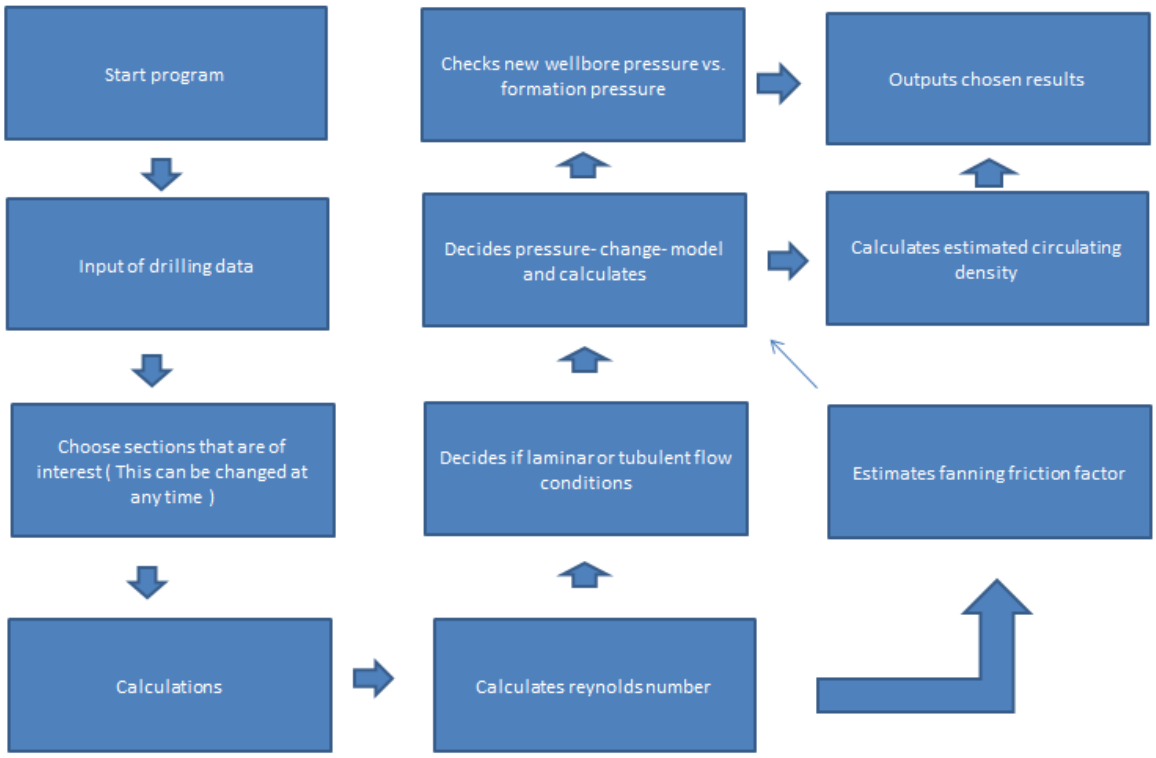

Figure 32: Flow chart for Program

6. Results

Due to lack of drilling data sensitivity analysis has been performed to see what parameters are effecting the pressure change the most. The drilling data that were provided are confidential, so that it was only possible to use some of the data. In chapter 4.2 and 4.3 the data used in the analysis is presented. For future work the model should be tested up towards real time drilling data.

6.1 Laminar flow sensitivity analysis

The sensitivity analyses done on the laminar flow equation gave good results. The results are based on the following equation derived in chapter 3.1.

$$\Delta p = \frac{q_{tot} * 2\Delta L}{\pi^2 * R^2 * \left(\frac{1}{\left(\frac{1}{n}\right)+1}(R - R_{DS})\right) * \left(R^2 - {R_{DS}}^2\right) * K} - \frac{v_{DS} * 2\Delta L}{\left(\frac{1}{\left(\frac{1}{n}\right)+1}(R - R_{DS})\right) * \left(R^2 - {R_{DS}}^2\right) * K}$$

Effective viscosity is set to 0,15 so we are operating in a laminar flow in the annulus and the Reynolds number is calculated to be $N_{Re} = 1728$.

When the velocity approaches zero, the flow approaches zero, hence the pressure drop approaches zero. When radius of the bottom hole assembly increases the pressure drop will increase also since the area of the flow decreases. Figure 33 below shows the pressure drop vs. the area of the annulus. The different areas are due to six different sizes of the bottom hole assembly, that gives different areas of the annulus. See appendix B for calculations.

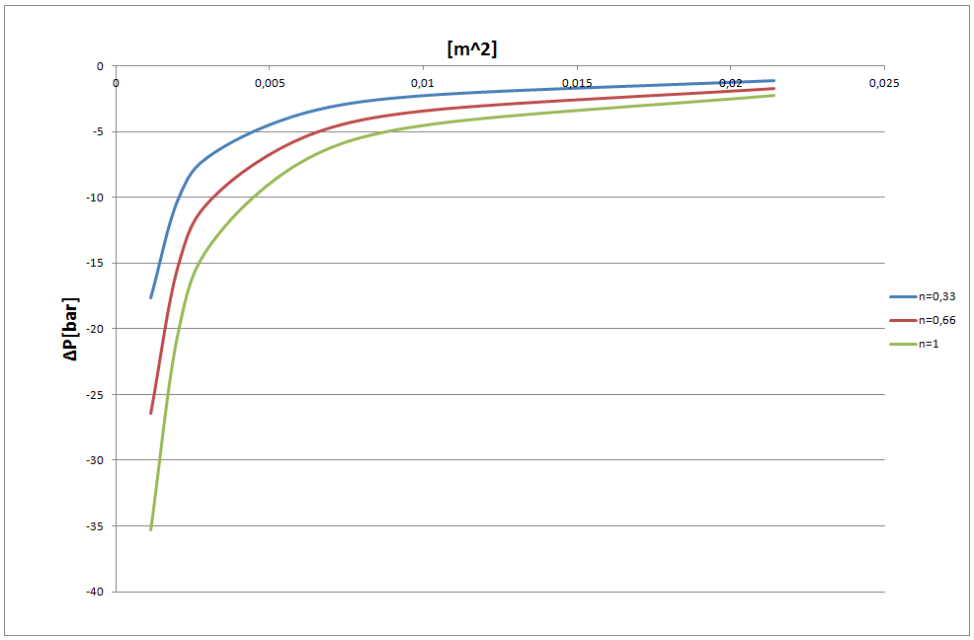

Figure 33: Flow area vs. Pressure loss

When looking at the pressure change due to the flow behavior index n at is observed that the pressure change is linear between 0,5 and 1,0. When the flow behavior index falls below 0,5 the pressure change increases rapidly. It is also mentionable to say that with a decreasing power law constant K, the pressure change decreases as well.

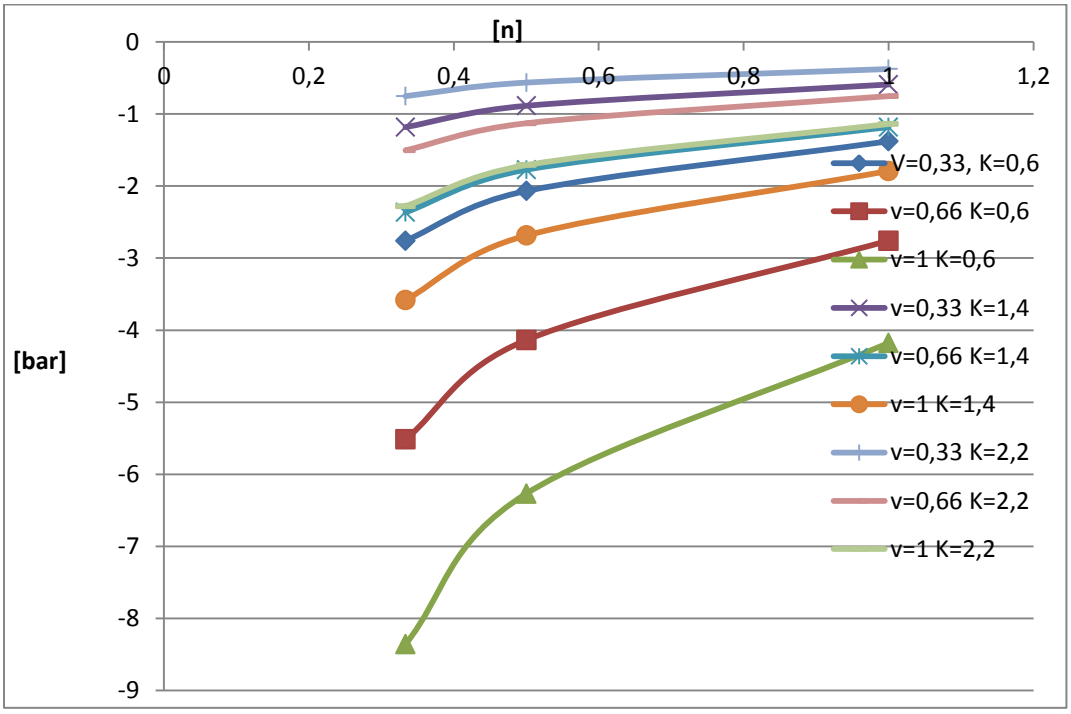

Figure 34: Pressure change vs n

It is a known fact that the pressure change depends on the velocity while tripping or running the drill string. Figure 35 shows how the pressure change develops when the speed is regulated between 0,33 m/s to 1 m/s. Low velocity and a high K-value gives the lowest pressure changes, and shown in the figure below the pressure change increases when increasing velocity and power law constant.

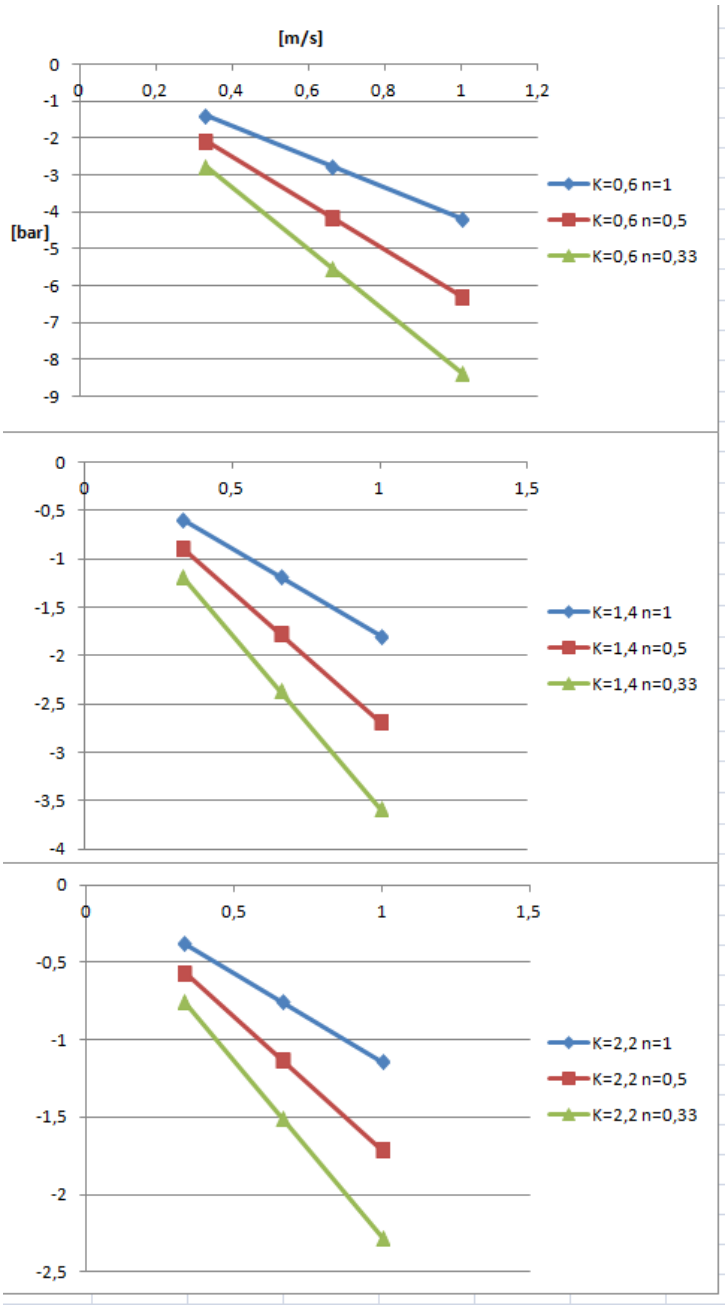

Figure 35: Velocity vs. Pressure change

6.2 Turbulent flow sensitivity analysis

The result from the sensitivity analysis on the turbulent flow equation gives good and realistic results. It is easy to see what parameters that affect the pressure change the most, hence what parameters that needs to be taken in to consideration when running or tripping.

Firstly the effects from the length of the section were tested. In the test the velocity and the fanning friction factor were changed, illustrated in figure 36, 37 and 38.

When the velocity of the pipe were set to 1 m/s the pressure change vary between 0,5 and 1,6 bar. When the length of the section increases the pressure change increases linearly.

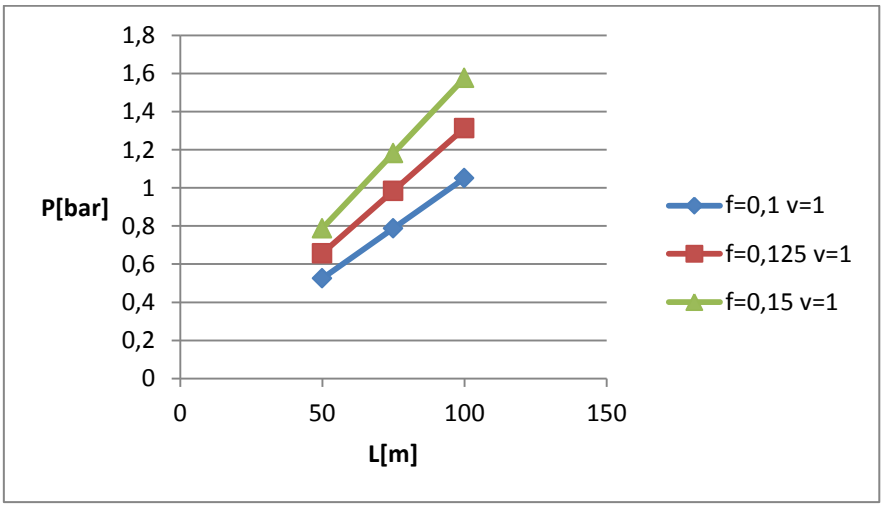

Figure 36: Length vs Pressure change, Velocity=1m/s

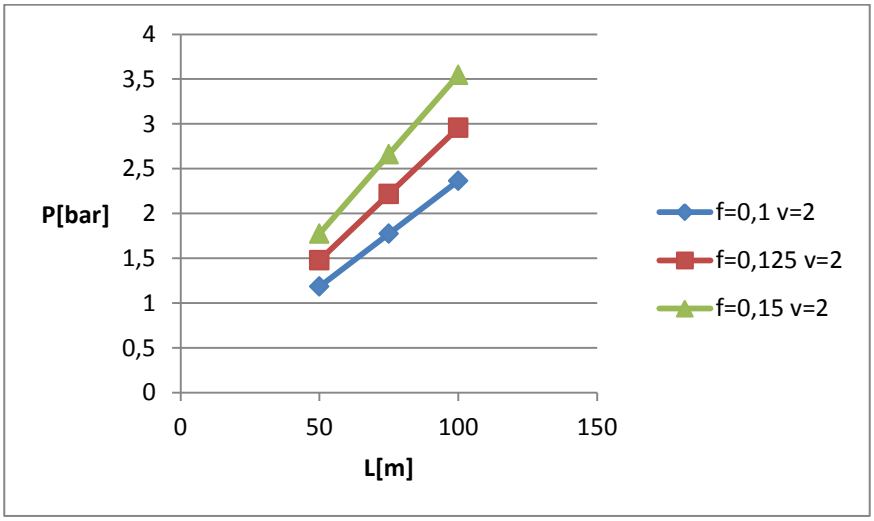

Figure 37: : Length vs Pressure change, Velocity=2m/s

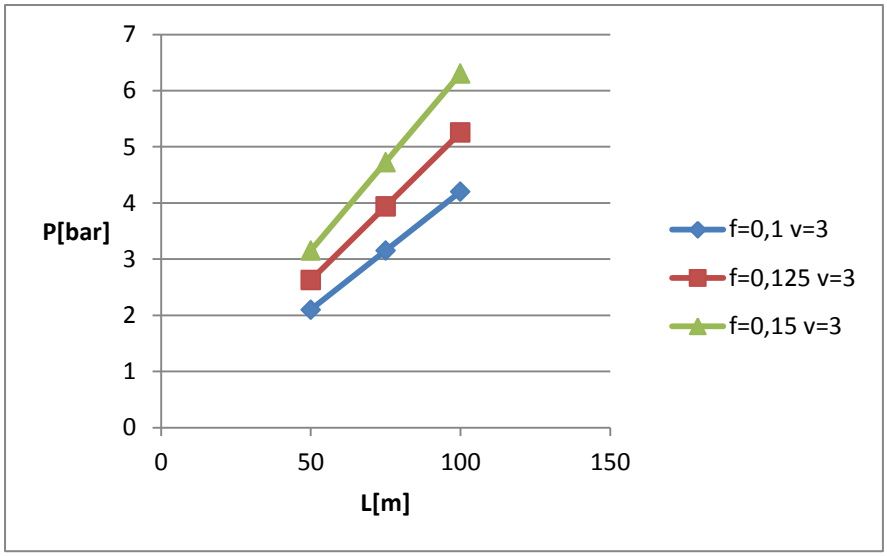

Figure 38: Length vs Pressure change, Velocity=3m/s

When velocity is tested at 3 m/s it gives and even higher pressure change. The pressure change can get as high as 6.3 bar with this speed. However the velocity is higher than what usually is used, and the fanning friction factor normally is lower than 0,15.

In figure 39, 40 and 41 velocity vs pressure change results are shown. As seen in the graphs the pressure change increases exponentially with increase in speed, unlike the length that is linear. This means that with high velocities the pressure increases rapidly.

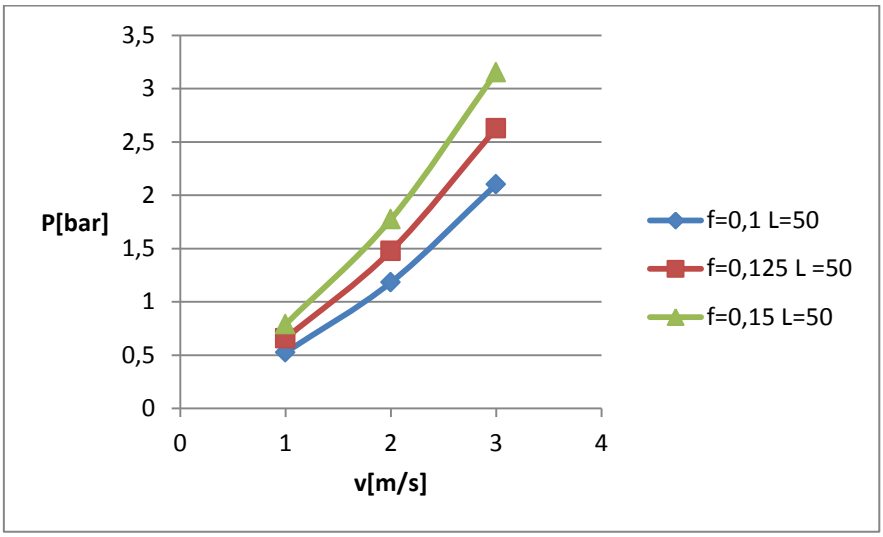

Figure 39: Velocity vs Pressure change, L=50m

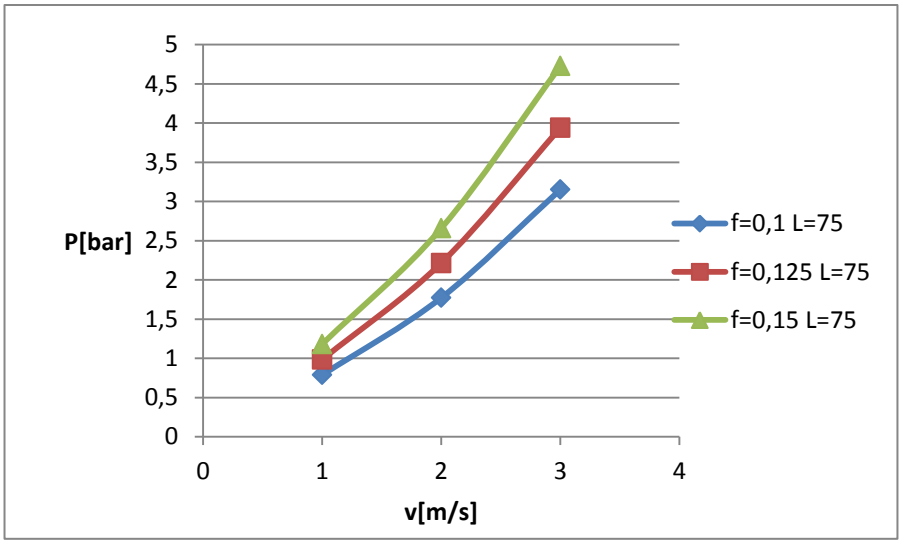

Figure 40: Velocity vs Pressure change, L=75m

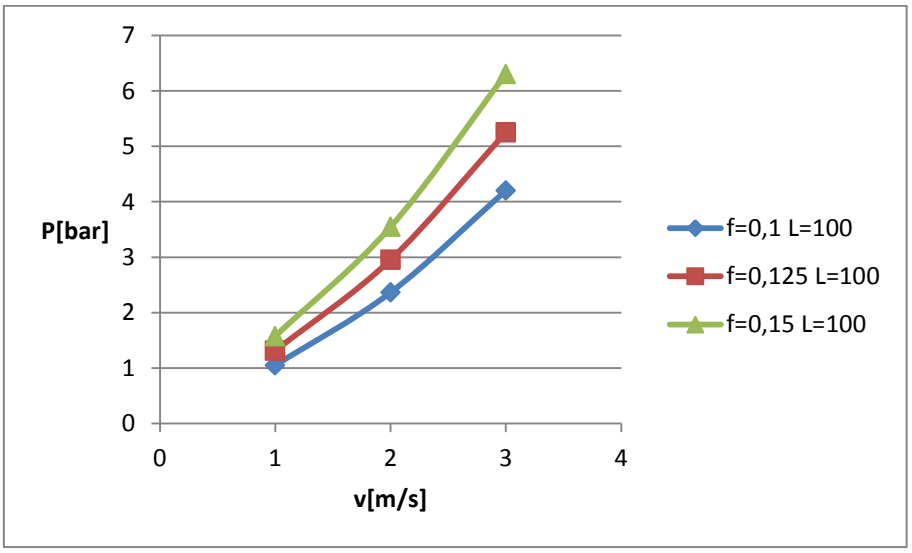

Figure 41: Velocity vs Pressure change, L=100m

As seen in the figures it is important to be careful when doing operations. The pressure changes increases fast, and in especially in a narrow mud window this can lead to damage of the wellbore. The velocity is the easiest parameter to handle, and the length and friction are parameters difficult to do anything about.

The diameter of the flow area is a factor that is important to take into consideration. Figure 38 and 39 shows diameter vs pressure change. The velocity is set to be 1m/s in analysis. As seen in the figures the pressure change decreases win increasing diameter. The decrease happens because the flow area becomes bigger. It is observed from the figures that the pressure change is linear in the start and down to around 0,11m, before it start to flatten out.

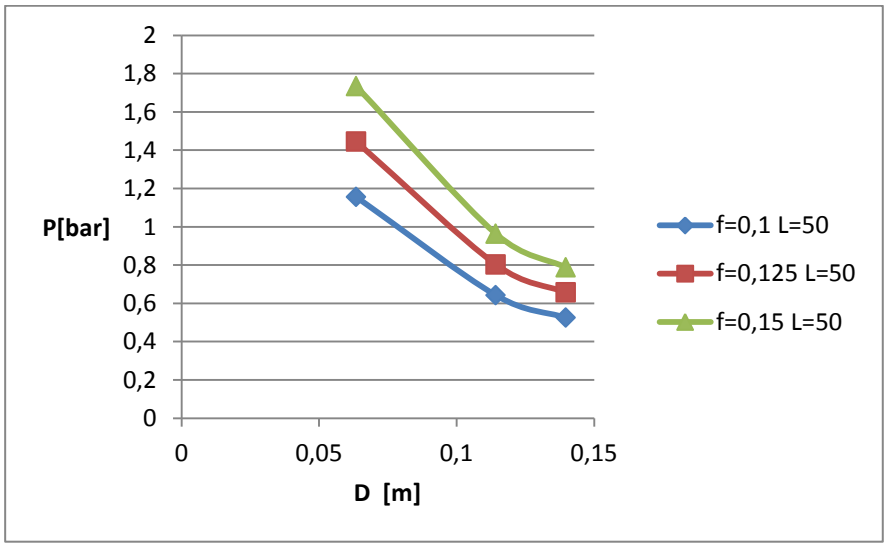

Figure 42: Diameter vs Pressure change L=50m, v=1 m/s

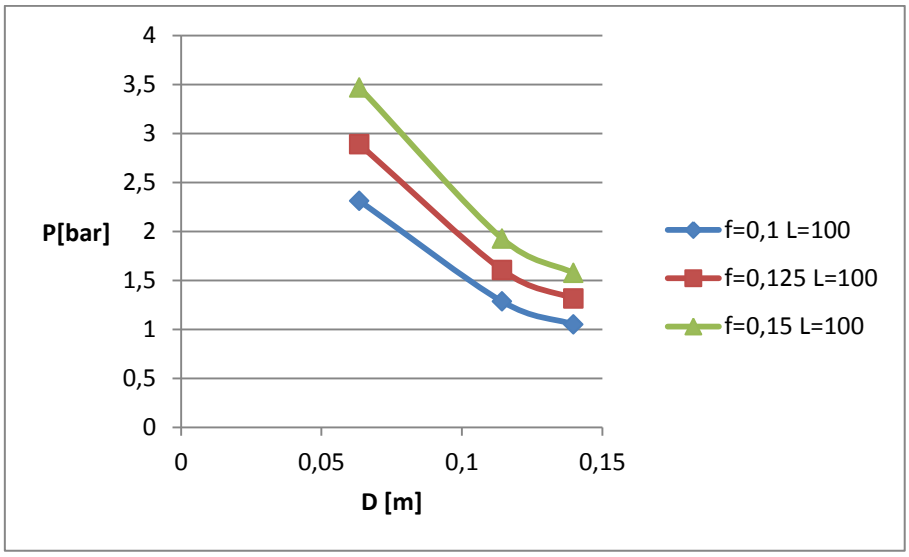

Figure 43: Diameter vs Pressure Change L=100m, v=1m/s

The diameter of the BHA or drill string must be taken in to consideration when operations are to happen. When the annuli area decreases the pressure change increases. Choosing a BHA or a drill sting with a smaller diameter can help keeping the changes at a minimum.

7. Discussion

The model published by Brooks in 1982 is discussed and adjusted in chapter 3.1 has been tested in EXCEL and MATLABT. The objective of this project was to improve the knowledge of surge and swab pressures and build a model that calculates these. The results presented in chapter 6 shows that this has been achieved. Brook's model have been further adjusted and translated into a MATLAB script and an Excel program that calculates the pressure drop. The MATLAB script can be found in Appendix C. The model shows good result in laminar flow, The model also shows that the surge and swab pressures increases rapidly when the power law index K is low and when the flow behavior index n is below 0,5. The model shows that as the diameter of the BHA increases the area of the annulus decreases and the pressure drop increases.

Pressure change in turbulent flow has given good and realistic results. The model used in this thesis gives good an indication on the what pressure changes that can be expected. The results show that the pressure changes linearly when changing the length and exponentially when increasing the velocity. The pressure change decreases with increasing diameter.

7.1 Quality of model

The model gives good and realistic results under laminar and turbulent flow conditions. It is easy to change parameters to check results with for example other diameters on the piping, or change the tripping speed to find what needs to be done not to get a to high pressure change.

The shortcoming of the model is that it has not been properly tested properly. Since it has been difficult to get drilling data from the industry, the testing of the model has been done with fictive data with a basis of some data from the drilling report. However, the data tested with are realistic values that should be in good comparison with the data used in real operations.

7.2 Quality of data

Unfortunately, the model was not tested up against real time drilling data. All companies approached have confidential drilling reports, and were not willing to share. The drilling report provided was a confidential internal document that could be used to get realistic values for the sensitivity analysis.

7.3 Future work

For future work it would be of interest to test the model with real drilling data, this to ensure that the results are good and within what is realistic. Companies need to provide drilling data from historical wells.It is easier to see what parameters affect the results when more tests have been made available.

The cling factor is a factor that we know little about, and it would be interesting to get a better understanding of this area. A closer study of the clinging of mud to the drill string can be of great importance, especially in future narrow wells.

To make the program more professional the program can be transformed from the EXCEL document it now is, into user friendly software.

8. Conclusion

Based on the results and evaluations the conclusions about Surge and swab pressure changes are as follows:

- In laminar flow the velocity of drilling operations as tripping or running the drill string is of great importance to the pressure change. Pressure change is dependent on the diameter and length of Bottom Hole Assembly or Drill string The larger the BHA diameter or drill string, the higher the pressure change gets. R-Rds -> 0 then $\Delta P \rightarrow \infty$

  When the Flow Behavior Index n gets smaller than 0,5 a rapid increase in pressure change occurs. Decreasing Power Law Constant K gives an increasing pressure change.
- In turbulent flow the velocity of the drill string and the mud is of great importance for calculating the pressure change. The pressure change increases exponentially with increased velocity. The length of the section gives a linear change in pressure, and the pressure change is also depended on the annular space. Increased fanning friction factor leads to ha higher pressure.
- To reduce the pressure changes it is important to manage the velocity and the diameter of the drill sting or BHA.
- The model is a useful tool to calculate pressure change and equivalent circulating density in a well. Both laminar- and turbulent flow models gives realistic results. However, the model is compared and tested towards real time drilling data.
- The model needs to be tested and compared with real time drilling data.
- The cling factor should be studied, and be included in the program if possible. The effects of the cling factor may change the results.

Nomenclature

Parameters

a	Constant
A	Area
b	constant
C1	Constant
C2	Constant
D	Diameter
f	Friction
F	Fanning friction factor
I	Inclination
K	Power Law Constant
K_C	Cling Constant
L	Length
n	Flow Behavior Index
P	Pressure
Q	Flow
R	Radius
Rc	Radius Cling
Rds	Radius of drill string
Rwell-	Radius of wellbore
v	Velocity
V	Volume
γ	Shear Rate
μ	Viscosity
τ	Share rate
p	Density

Abbreviations

BHA	Bottom Hole Assembly
ECD	Equivalent Circulating Density
He	Total vertical elevation
Hf	Frictional head
NAF	Non Aqueous Fluids
NOV	National Oilwell Varco
OMD	Oil Based Mud
Re	Reynolds number
RPM	Rotations Per Minute
TH	Total Head
WBM	Water Based Mud

Reference list:

Brooks, A.G. (1982). Swab and Surge Pressures in Non-Newtonian Fluids. Exploration Logging Inc.

Burkhardt, J. A. (1961). Wellbore pressure surges produced by pipe movement. Journal of petroleum technology, 13 (6), 595-605.

Bourgoyne, A. T., Millheim, K. K., Chenevert, M. E., & Young, F. S. (1986).Applied drilling engineering (2nd ed.; J. F. Evers & D. S. Pye, Eds.). Society of Petroleum Engineers.

Adebayo and Chinonyere (2012). Sawdust As A Filtration Control And Density Additives in Water Based Drilling Mud. International Journal of Scientific & Engineering Research

Schubert, J.(2010). Well Controll , Society of Petroleum Engineers.

Cannon, G. E. (1934). Changes in hydrostatic pressure during withdrawing of drillpipe from the hole. In Presented at spring meeting. Southwestern district. fort worth. Texas. April 1034. (Vol. 1, p. 7).

Mitchell, R. F. (1988, September). Dynamic surge/swab pressure predictions. SPE Drilling engineering, 3 (3), 325-333.

Mitchell, R. F. (2004). Surge pressures in low-clearance liners. In Iadc/spe drilling conference, 2-4 march 2004, Dallas, Texas (p. 9). Society of Petroleum Engineers. (Document ID87181-MS)

Gjerstad, Time, BjørkVoll. (2013). A Medium-Order Flow Model for Dynamic Pressure Surges in Tripping Operations. Society of Petroleum Engineers

R. Srivastav, F. C. R. A. A. S., M. En_s. (2012). Surge and swab pressures in horizontal and inclined wells. In Spe latin america and Caribbean petroleum engineering conference, 16-18 april 2012, mexico city, Mexico (Vol. 1, p. 8).

Crespo, Ahmed, Enfis, Saasen, Amani (2012). Surge and Swab Pressure Predictions for Yield-Power-Law Drilling Fluids. Seciety of Petroleum Engineers

Skalle, P. (2012). Drilling fluid engineering. Ventus publishing Aps.

Oil, S., & gas dictionary. Retrieved from http://www.glossary.oilfield.slb.com

Naley.H (2012). Swab pressures determined experimentally and theoretically

Haliburton. (2012). Lost circulation Retrieved from :http://www.halliburton.com/public/cem/contents/Overview/images/flexplug.gif

Celtiqueenergie (2014) Retrieved from: [http://www.celtiqueenergie.com/Uploads/Geological-Survey-Frac-v3-3Z1334156142.jpg]

Nial Barker(2010) Retrieved from http://blog.nialbarker.com/wpcontent/uploads/2010/03/laminar_turbulent_flow.gif

Enigineeringtoolbox (2014) Retrieved from: http://www.engineeringtoolbox.com/laminar-transitional-turbulent-flow-d_577.html

ODP(2010) Retrieved from:

[http://www-odp.tamu.edu/publications/tnotes/tn31/ris/images/ris_1.jpg, EditedAndreas Grav Karlsen]

Aliimg (2010) Retrieved from: http://i01.i.aliimg.com/photo/v0/108779901/Mud_Balance.jpg

Survey (2005). Retrieved from http://people.sju.edu/~phabdas/physics/viscosity2.gif

Solutions(2014). Retrieved from http://solutions.3m.com/3MContentRetrievalAPI/BlobServlet?lmd=1342614075000&locale=en_WW&assetType=MMM_Image&assetId=1319233768969&blobAttribute=ImageFile

Airdrilling (2012). Retrieved from: http://www.airdrilling.com/images/underbalanced-drilling.jpg

Appendix A

Appendix A gives an overview of how the different calculations and inputs are set up in the EXCEL calculator. Pictures from the program with a short description are added.

Description of program:

The main sheet is the sheet that needs input filled in. Information from the different well sections are to be inserted and the values desired to be calculated will be shown in the “Output” side of the sheet. The user can decide what information they want, and what sections of the well they want to take a closer look at. All the calculations are done in linked sheets that you can see beneath.

Surge and Swab Pressure Calculator

(Only change cells marked in yellow)

Input data

General information			
Diameter Drill Sting	Dds	0,1397	[m]
Mud denisty	ρ	1200	[kg/m^3]
Formation pressure	Pform	320	[bar]
Wellbore pressure	Pwell	350	[bar]
Pi		3,14	

Section 1:		In use (YES or NO):	YES
Drill Sting Diameter	Dds	0,1397	[m]
Borehole Diameter	Dwell	0,3048	[m]
Diamter Annulus	Dann	0,1651	[m]
Mud Density	ρ	1200	[kg/m^3]
Velocity drill string	v	0,46734349	[m/s]
Dynamic Viscosity	μ	0,0042	[Pa*s]
Length of Section	L	50	[m]
Flow	Qtot	0,01	[m^3/s]
Area wellbore	Aw	0,07292889	[m^2]
Area Drillstring	Ads	0,01532013	[m^2]
Area Annulus	Aann	0,02139754	[m^2]
Power law constant	K	1	
Flow behavior index	n	0,33	
Fanning friction factor	f	0,10239717	
Velocity fluid	Up	0,1	[m/s]

Section 2:		In use (YES or NO):	YES
Drill Sting Diameter	Dds	0,1397	[m]
Borehole Diameter	Dwell	0,2413	[m]
Diamter Annulus	Dann	0,1016	[m]
Mud Density	ρ	1200	[kg/m^3]
Velocity drill string	v	1,2340789	[m/s]
Dynamic Viscosity	μ	0,0042	[Pa*s]
Length of Section	L	500	[m]
Flow	Qtot	0,01	[m^3/s]
Area wellbore	Aw	0,04570717	[m^2]
Area Drillstring	Ads	0,01532013	[m^2]
Area Annulus	Aann	0,00810321	[m^2]
Power law constant	K	1	
Flow behavior index	n	0,33	
Fanning friction factor	f	0,10211321	
Velocity fluid	Up	0,1	[m/s]

Section 3:		In use (YES or NO):	YES
Drill Sting Diameter	Dds	0,1397	[m]
Borehole Diameter	Dwell	0,2032	[m]
Diamter Annulus	Dann	0,0635	[m]
Mud Density	ρ	1200	[kg/m^3]
Velocity drill string	v	3,15924199	[m/s]
Dynamic Viscosity	μ	0,0042	[Pa*s]
Length of Section	L	900	[m]
Flow	Qtot	0,01	[m^3/s]
Area wellbore	Aw	0,03241284	[m^2]
Area Drillstring	Ads	0,01532013	[m^2]
Area Annulus	Aann	0,00316532	[m^2]
Power law constant	K	1	
Flow behavior index	n	0,33	
Fanning friction factor	f	0,10194234	
Velocity fluid	Up	0,1	[m/s]

Section 4:		In use (YES or NO):	YES
Drill Sting Diameter	Dds	0,1397	[m]
Borehole Diameter	Dwell	0,2032	[m]
Diamter Annulus	Dann	0,0635	[m]
Mud Density	ρ	1200	[kg/m^3]
Velocity drill string	v	3,15924199	[m/s]
Dynamic Viscosity	μ	0,0042	[Pa*s]
Length of Section	L	300	[m]
Flow	Qtot	0,01	[m^3/s]
Area wellbore	Aw	0,03241284	[m^2]
Area Drillstring	Ads	0,15320131	[m^2]
Area Annulus	Aann	0,00316532	[m^2]
Power law constant	K	1	
Flow behavior index	n	0,33	
Fanning friction factor	f	0,10194234	
Velocity fluid	Up	0,1	[m/s]

Section 5:		In use (YES or NO):	YES
Drill Sting Diameter	Dds	0,1397	[m]
Borehole Diameter	Dwell	0,2032	[m]
Diamter Annulus	Dann	0,0635	[m]
Mud Density	ρ	1200	[kg/m^3]
Velocity drill string	v	2,39614006	[m/s]
Dynamic Viscosity	μ	0,0042	[Pa*s]
Length of Section	L	200	[m]
Flow	Qtot	0,01	[m^3/s]
Area wellbore	Aw	0,0427354	[m^2]
Area Drillstring	Ads	0,01532013	[m^2]
Area Annulus	Aann	0,00417338	[m^2]
Power law constant	K	1	
Flow behavior index	n	0,33	
Fanning friction factor	f	0,10203308	
Velocity fluid	Up	0,1	[m/s]

Section BHA:		In use (YES or NO):	YES
Drill Sting Diameter	Dds	0,1524	[m]
Borehole Diameter	Dwell	0,2032	[m]
Diamter Annulus	Dann	0,0508	[m]
Mud Density	ρ	1200	[kg/m^3]
Velocity drill string	v	4,93631561	[m/s]
Dynamic Viscosity	μ	0,0042	[Pa*s]
Length of Section	L	75	[m]
Flow	Qtot	0,01	[m^3/s]
Area wellbore	Aw	0,03241284	[m^2]
Area Drillstring	Ads	0,01823222	[m^2]
Area Annulus	Aann	0,0020258	[m^2]
Power law constant	K	1	
Flow behavior index	n	0,33	
Fanning friction factor	f	0,10188531	
Velocity fluid	Up	0,1	[m/s]

Output

Output for the calculation sheet

Surge and Swab Pressure Change			
Pressure Loss over BHA	YES	3,111401	[bar]
Pressure Loss over the drill string:	NO		[bar]
Total pressure change due to Surge and swab is:		3,111401	[bar]

New Pressure in wellbore, when pressure change is added		
Bottom hole pressure	350	[bar]
Total pressure change due to Surge and swab is:	3,111401	[bar]
New bottom hole pressure:	353,1114	[bar]

Wellbore pressure is higher than formation pressure!!!!

Equivalent Circulating Density		YES
Section 1	YES	1205,884 [kg/m^3]
Section 2	YES	1375,155 [kg/m^3]
Section 3	YES	1472,599 [kg/m^3]
Section 4	YES	1631,167 [kg/m^3]
Section 5	YES	1670,268 [kg/m^3]
Section 6	YES	1758,804 [kg/m^3]

Main Sheet , EXCEL Program

This sheet calculates if the flow is laminar or turbulent. Further on the pressure loss is chosen from the two different calculations depending on the condition of the flow. All cells are in this sheet linked together so if you are to change one of them the rest will follow.

Calculations																			
Reynold number, Laminar if Re<2300, Turbulent if Re>2300																			
Section 1	22045,26	Turbulent																	
Section 2	35823,55	Turbulent																	
Section 3	57317,68	Turbulent																	
Section 4	57317,68	Turbulent																	
Section 5	43472,83	Turbulent																	
Section 6	71647,1	Turbulent																	
Pressure change due to surge and swab																			
Section 1																			
Section 2																			
Section 3																			
Section 4																			
Section 5																			

Turbulent pressure drop calulations										
Section 1	ΔP=	2885,99736	[Pa]	0,02886	[bar]					
Section 2	ΔP=	159133,2001	[Pa]	1,591332	[bar]					
Section 3	ΔP=	1706774,577	[Pa]	17,06775	[bar]					
Section 4	ΔP=	568924,8589	[Pa]	5,689249	[bar]					
Section 5	ΔP=	222666,4251	[Pa]	2,226664	[bar]					
Section BHA	ΔP=	311140,079	[Pa]	3,111401	[bar]					
Laminar pressure drop calculations										
Section 1	ΔP=	363,1470895	-	83,72317		279,42392	[Pa]	0,002794	[bar]	
Section 2	ΔP=	17850,54045	-	1894,984		15955,5562	[Pa]	0,159556	[bar]	
Section 3	ΔP=	128880,9021	-	7858,879		121022,023	[Pa]	1,21022	[bar]	
Section 4	ΔP=	42960,30069	-	2619,626		40340,6745	[Pa]	0,403407	[bar]	
Section 5	ΔP=	28640,20046	-	1324,578		27315,6229	[Pa]	0,273156	[bar]	
Section BHA	ΔP=	16182,0329	-	1061,191		15120,8417	[Pa]	0,151208	[bar]	
	Section 1 Turbulent	Section 2 Turbulent	Section 3 Turbulent	Section 4 Turbulent	Section 5 Turbulent	Section BHA Turbulent		Total ΔP DS	Total ΔP BHA	
	0,02885997	1,591332001	17,06775	5,689249	2,226664	3,11140079		26,60385	3,111401	

Pressure loss Sheet

The following sheet gives a calculation of the fanning factor. The sheet is connected up towards the calculation of the Reynolds number and gives the value of the fanning factor for the desired sector. Calculations are done for each sector and are linked up to calculate the pressure change in the sections that are turbulent. This calculation is developed by [nn] and small changes are done to it in this thesis.

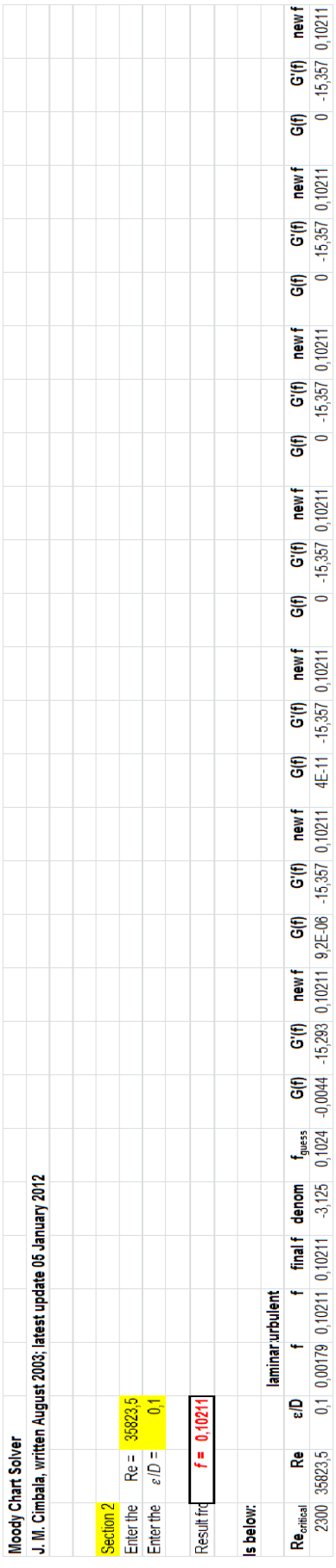

Moody Chart Solver																													
J. M. Cimbala, written August 2003; latest update 06 January 2012																													
Section 2																													
Enter the	Re =	35823,5																											
Enter the	ε/D =	0,1																											
Result fro	f =	0,10211																											
Is below:																													
			laminar:urbulent																										
$Re_{critical}$	Re	ε/D	f	f	final f	denom	f_{guess}	G(f)	G'(f)	new f	G(f)	G'(f)	new f	G(f)	G'(f)	new f	G(f)	G'(f)	new f	G(f)	G'(f)	new f	G(f)	G'(f)	new f	G(f)	G'(f)	new f	G(f)	G'(f)	new f
2300	35823,5	0,1	0,00179	0,10211	0,10211	-3,125	0,1024	-0,0044	-15,293	0,10211	9,2E-06	-15,357	0,10211	4E-11	-15,357	0,10211	0	-15,357	0,10211	0	-15,357	0,10211	0	-15,357	0,10211	0	-15,357	0,10211	0	-15,357	0,10211

Fanning factor Calculator

The ECD calculations are in a separate sheet. Calculations for the ECD are done for each section. The calculations are based on the work of associate professor Pål Skalle. The pressure change due to rotation and acceleration are in this thesis neglected, due to the complexity of this.

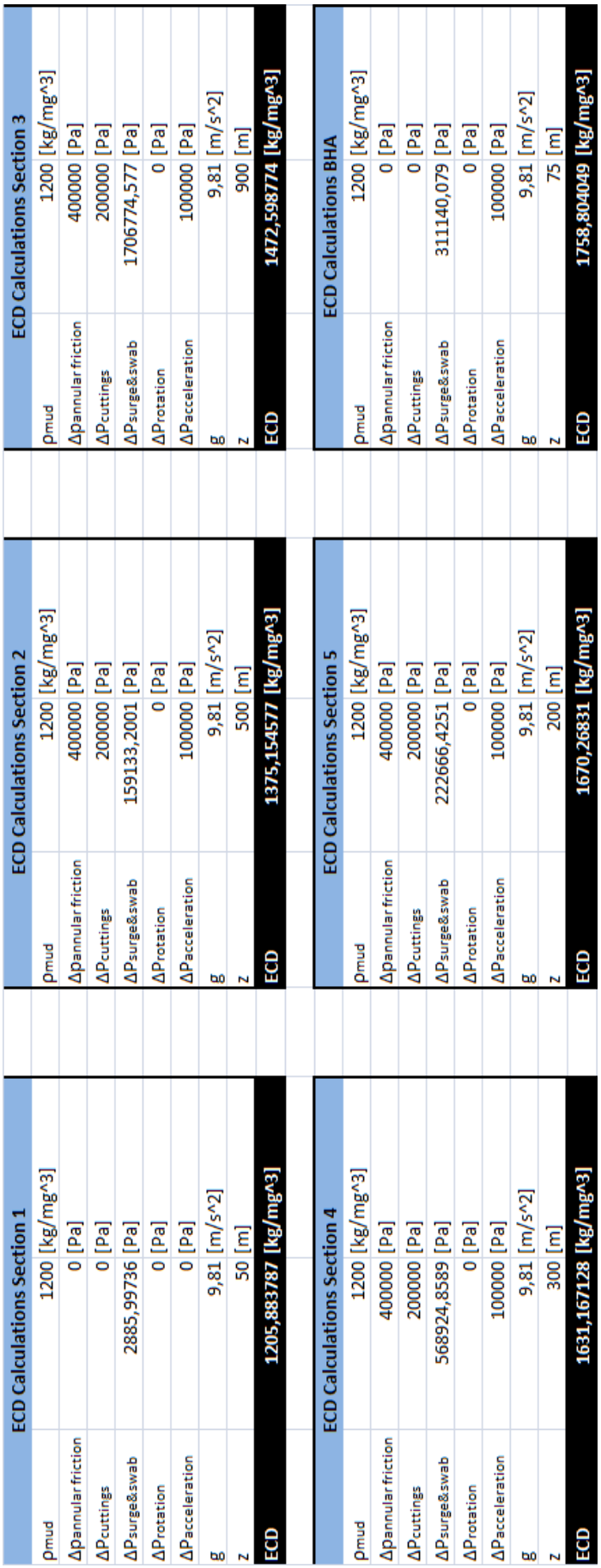

ECD Calculations Section 1	
ρ_{mud}	1200 [kg/mg^3]
$\Delta p_{annular\ friction}$	0 [Pa]
$\Delta P_{cuttings}$	0 [Pa]
$\Delta P_{surge\&swab}$	2885,99736 [Pa]
$\Delta P_{rotation}$	0 [Pa]
$\Delta P_{acceleration}$	0 [Pa]
g	9,81 [m/s^2]
z	50 [m]
ECD	1205,883787 [kg/mg^3]

ECD Calculations Section 2	
ρ_{mud}	1200 [kg/mg^3]
$\Delta p_{annular\ friction}$	400000 [Pa]
$\Delta P_{cuttings}$	200000 [Pa]
$\Delta P_{surge\&swab}$	159133,2001 [Pa]
$\Delta P_{rotation}$	0 [Pa]
$\Delta P_{acceleration}$	100000 [Pa]
g	9,81 [m/s^2]
z	500 [m]
ECD	1375,154577 [kg/mg^3]

ECD Calculations Section 3	
ρ_{mud}	1200 [kg/mg^3]
$\Delta p_{annular\ friction}$	400000 [Pa]
$\Delta P_{cuttings}$	200000 [Pa]
$\Delta P_{surge\&swab}$	1706774,577 [Pa]
$\Delta P_{rotation}$	0 [Pa]
$\Delta P_{acceleration}$	100000 [Pa]
g	9,81 [m/s^2]
z	900 [m]
ECD	1472,598774 [kg/mg^3]

ECD Calculations Section 4	
ρ_{mud}	1200 [kg/mg^3]
$\Delta p_{annular\ friction}$	400000 [Pa]
$\Delta P_{cuttings}$	200000 [Pa]
$\Delta P_{surge\&swab}$	568924,8589 [Pa]
$\Delta P_{rotation}$	0 [Pa]
$\Delta P_{acceleration}$	100000 [Pa]
g	9,81 [m/s^2]
z	300 [m]
ECD	1631,167128 [kg/mg^3]

ECD Calculations Section 5	
ρ_{mud}	1200 [kg/mg^3]
$\Delta p_{annular\ friction}$	400000 [Pa]
$\Delta P_{cuttings}$	200000 [Pa]
$\Delta P_{surge\&swab}$	222666,4251 [Pa]
$\Delta P_{rotation}$	0 [Pa]
$\Delta P_{acceleration}$	100000 [Pa]
g	9,81 [m/s^2]
z	200 [m]
ECD	1670,26831 [kg/mg^3]

ECD Calculations BHA	
ρ_{mud}	1200 [kg/mg^3]
$\Delta p_{annular\ friction}$	0 [Pa]
$\Delta P_{cuttings}$	0 [Pa]
$\Delta P_{surge\&swab}$	311140,079 [Pa]
$\Delta P_{rotation}$	0 [Pa]
$\Delta P_{acceleration}$	100000 [Pa]
g	9,81 [m/s^2]
z	75 [m]
ECD	1758,804049 [kg/mg^3]

ECD Calculations

Appendix B

Sensitivity analyses:

The sensitivity analyses is based on the two equation presented in chapter 3. For the laminar and the turbulent analysis three parameters have been tested. The other parameters have been set to realistic values.

$$\Delta p = \frac{q_{tot} * 2\Delta L}{\pi^2 * R^2 * \left(\frac{1}{\left(\frac{1}{n}\right)+1}(R-R_{DS})\right) * \left(R^2 - {R_{DS}}^2\right) * K} - \frac{v_{DS} * 2\Delta L}{\left(\frac{1}{\left(\frac{1}{n}\right)+1}(R-R_{DS})\right) * \left(R^2 - {R_{DS}}^2\right) * K} \quad (42)$$

$$\Delta P_s = 2f * \frac{\rho {(u_p + V_p)}^2}{g_c * d_{p,i}} * L \quad [44]$$

Case	f	L	vds	dP
1	0,1	50	1	0,52537
4	0,1	75	1	0,78806
7	0,1	100	1	1,05074
Case	f	L	vds	dP
10	0,125	50	1	0,65672
13	0,125	75	1	0,98507
16	0,125	100	1	1,31343
Case	f	L	vds	dP
19	0,15	50	1	0,78806
22	0,15	75	1	1,18209
25	0,15	100	1	1,57612
Case	f	L	vds	dP
2	0,1	50	2	1,18209
5	0,1	75	2	1,77313
8	0,1	100	2	2,36417
11	0,125	50	2	1,47761
14	0,125	75	2	2,21641
17	0,125	100	2	2,95522
20	0,15	50	2	1,77313
23	0,15	75	2	2,6597
26	0,15	100	2	3,54626
Case	f	L	vds	dP
3	0,1	50	3	2,10149
6	0,1	75	3	3,15223
9	0,1	100	3	4,20298
12	0,125	50	3	2,62686
15	0,125	75	3	3,94029
18	0,125	100	3	5,25372
21	0,15	50	3	3,15223
24	0,15	75	3	4,72835
27	0,15	100	3	6,30447

V = 0,33

Case	K	n	vds	Qtot	dP
1	0,6	1	0,33	0,007061	-1,37909
4	0,6	0,5	0,33	0,007061	-2,06864
7	0,6	0,333333	0,33	0,007061	-2,75818
10	1,4	1	0,33	0,007061	-0,59104
13	1,4	0,5	0,33	0,007061	-0,88656
16	1,4	0,333333	0,33	0,007061	-1,18208
19	2,2	1	0,33	0,007061	-0,37612
22	2,2	0,5	0,33	0,007061	-0,56417
25	2,2	0,333333	0,33	0,007061	-0,75223

V = 0,66

Case	K	n	vds	Qtot	dP
2	0,6	1	0,66	0,014122	-2,75818
5	0,6	0,5	0,66	0,014122	-4,13727
8	0,6	0,333333	0,66	0,014122	-5,51637
11	1,4	1	0,66	0,014122	-1,18208
14	1,4	0,5	0,66	0,014122	-1,77312
17	1,4	0,333333	0,66	0,014122	-2,36416
20	2,2	1	0,66	0,014122	-0,75223
23	2,2	0,5	0,66	0,014122	-1,12835
26	2,2	0,333333	0,66	0,014122	-1,50446

V=1,0

Case	K	n	vds	Qtot	dP
3	0,6	1	1	0,021398	-4,17906
6	0,6	0,5	1	0,021398	-6,2686
9	0,6	0,333333	1	0,021398	-8,35813
12	1,4	1	1	0,021398	-1,79103
15	1,4	0,5	1	0,021398	-2,68654
18	1,4	0,333333	1	0,021398	-3,58206
21	2,2	1	1	0,021398	-1,13974
24	2,2	0,5	1	0,021398	-1,70962
27	2,2	0,333333	1	0,021398	-2,27949

Case	K	n	vds	Qtot	dP	Case	K	n	vds	Qtot	dP	Case	K	n	vds	Qtot	dP
1	0,6	1	0,33	0,007061	-1,37909	2	0,6	1	0,66	0,014122	-2,75818	3	0,6	1	1	0,021398	-4,17906
4	0,6	0,5	0,33	0,007061	-2,06864	5	0,6	0,5	0,66	0,014122	-4,13727	6	0,6	0,5	1	0,021398	-6,2686
7	0,6	0,333333	0,33	0,007061	-2,75818	8	0,6	0,333333	0,66	0,014122	-5,51637	9	0,6	0,333333	1	0,021398	-8,35813
10	1,4	1	0,33	0,007061	-0,59104	11	1,4	1	0,66	0,014122	-1,18208	12	1,4	1	1	0,021398	-1,79103
13	1,4	0,5	0,33	0,007061	-0,88656	14	1,4	0,5	0,66	0,014122	-1,77312	15	1,4	0,5	1	0,021398	-2,68654
16	1,4	0,333333	0,33	0,007061	-1,18208	17	1,4	0,333333	0,66	0,014122	-2,36416	18	1,4	0,333333	1	0,021398	-3,58206
19	2,2	1	0,33	0,007061	-0,37612	20	2,2	1	0,66	0,014122	-0,75223	21	2,2	1	1	0,021398	-1,13974
22	2,2	0,5	0,33	0,007061	-0,56417	23	2,2	0,5	0,66	0,014122	-1,12835	24	2,2	0,5	1	0,021398	-1,70962
25	2,2	0,333333	0,33	0,007061	-0,75223	26	2,2	0,333333	0,66	0,014122	-1,50446	27	2,2	0,333333	1	0,021398	-2,27949

Calculations with

different diameters.

8,5'' Hole diameter with different BHA sizes K=2,2, v=1

6'' BHA		
R	0,108	m
Rds	0,076	m
dL	70,000	m
Areal,A	0,00317	m^2
Pi	3,14	

Case	K	n	vds	Qtot	dP
19	2,2	1	1	0,00317	-6,6672
22	2,2	0,5	1	0,00317	-10,0008
25	2,2	0,33333	1	0,00317	-13,3344

5'' BHA		
R	0,108	m
Rds	0,064	m
dL	70,000	m
Areal,A	0,0062	m^2
Pi	3,14	

Case	K	n	vds	Qtot	dP
19	2,2	1	1	0,0062	-3,55424
22	2,2	0,5	1	0,0062	-5,33136
25	2,2	0,33333	1	0,0062	-7,10848

6,5'' BHA		
R	0,108	m
Rds	0,083	m
dL	70,000	m
Areal,A	0,00203	m^2
Pi	3,14	

Case	K	n	vds	Qtot	dP
19	2,2	1	1	0,00203	-10,173
22	2,2	0,5	1	0,00203	-15,2594
25	2,2	0,33333	1	0,00203	-20,3459

4''BHA		
R	0,108	m
Rds	0,051	m
dL	70,000	m
Areal,A	0,01026	m^2
Pi	3,14	

Case	K	n	vds	Qtot	dP
19	2,2	1	1	0,01026	-2,23555
22	2,2	0,5	1	0,01026	-3,35332
25	2,2	0,33333	1	0,01026	-4,47109

7'' BHA		
R	0,108	m
Rds	0,089	m
dL	70,000	m
Areal,A	0,00114	m^2
Pi	3,14	

Case	K	n	vds	Qtot	dP
19	2,2	1	1	0,00114	-17,6393
22	2,2	0,5	1	0,00114	-26,4589
25	2,2	0,33333	1	0,00114	-35,2786

2''BHA		
R	0,108	m
Rds	0,025	m
dL	70,000	m
Areal,A	0,0214	m^2
Pi	3,14	

Case	K	n	vds	Qtot	dP
19	2,2	1	1	0,0214	-1,13974
22	2,2	0,5	1	0,0214	-1,70962
25	2,2	0,33333	1	0,0214	-2,27949

K	n	vds	Qtot	dP
2,2	1	1	0,00114	-17,6393
2,2	1	1	0,00203	-10,173
2,2	1	1	0,00317	-6,6672
2,2	1	1	0,0062	-3,55424
2,2	1	1	0,01026	-2,23555
2,2	1	1	0,0214	-1,13974

K	n	vds	Qtot	dP
2,2	0,5	1	0,00114	-26,4589
2,2	0,5	1	0,00203	-15,2594
2,2	0,5	1	0,00317	-10,0008
2,2	0,5	1	0,0062	-5,33136
2,2	0,5	1	0,01026	-3,35332
2,2	0,5	1	0,0214	-1,70962

K	n	vds	Qtot	dP
2,2	0,33333	1	0,00114	-35,2786
2,2	0,33333	1	0,00203	-20,3459
2,2	0,33333	1	0,00317	-13,3344
2,2	0,33333	1	0,0062	-7,10848
2,2	0,33333	1	0,01026	-4,47109
2,2	0,33333	1	0,0214	-2,27949

The turbulent analysis:

Sensitivity Analysis Turbulent

ρ	1800,000	kg/m3	0,1	
vds	1,000	m/s	Re	1143
up	1,000	m/s		
g	9,81			

$$\Delta P_s = 2f\frac{\rho(u_p + V_p)^2}{g_c d_{p,j}}L.$$

	f	L	dds	dP
	[]	(-)	[m]	(bar)
a	0,1	50,000	0,06	
b	0,125	75,000	0,11	
c	0,15	100,000	0,14	

Test Matrix Set-up

Case	K	n	vds
1	a	a	a
2	a	a	b
3	a	a	c
4	a	b	a
5	a	b	b
6	a	b	c
7	a	c	a
8	a	c	b
9	a	c	c
10	b	a	a
11	b	a	b
12	b	a	c
13	b	b	a
14	b	b	b
15	b	b	c
16	b	c	a
17	b	c	b
18	b	c	c
19	c	a	a
20	c	a	b
21	c	a	c
22	c	b	a
23	c	b	b
24	c	b	c
25	c	c	a
26	c	c	b
27	c	c	c

Simulation

Sensitivity

Case	f	L	vds	dP
1	0,1	50	0,0635	1,1558188
2	0,1	50	0,1143	0,6421216
3	0,1	50	0,1397	0,5253722
4	0,1	75	0,0635	1,7337282
5	0,1	75	0,1143	0,9631824
6	0,1	75	0,1397	0,7880583
7	0,1	100	0,0635	2,3116377
8	0,1	100	0,1143	1,2842431
9	0,1	100	0,1397	1,0507444
10	0,125	50	0,0635	1,4447735
11	0,125	50	0,1143	0,802652
12	0,125	50	0,1397	0,6567152
13	0,125	75	0,0635	2,1671603
14	0,125	75	0,1143	1,2039779
15	0,125	75	0,1397	0,9850729
16	0,125	100	0,0635	2,8895471
17	0,125	100	0,1143	1,6053039
18	0,125	100	0,1397	1,3134305
19	0,15	50	0,0635	1,7337282
20	0,15	50	0,1143	0,9631824
21	0,15	50	0,1397	0,7880583
22	0,15	75	0,0635	2,6005924
23	0,15	75	0,1143	1,4447735
24	0,15	75	0,1397	1,1820874
25	0,15	100	0,0635	3,4674565
26	0,15	100	0,1143	1,9263647
27	0,15	100	0,1397	1,5761166

Velocity calculations

Case	K	n	vds	Qtot	dP	Case	K	n	vds	Qtot	dP
4	0,6	0,5	0,33	0,00706	-2,06864	7	0,6	0,33333	0,33	0,00706	-2,75818
5	0,6	0,5	0,66	0,01412	-4,13727	8	0,6	0,33333	0,66	0,01412	-5,51637
6	0,6	0,5	1	0,0214	-6,2686	9	0,6	0,33333	1	0,0214	-8,35813
13	1,4	0,5	0,33	0,00706	-0,88656	16	1,4	0,33333	0,33	0,00706	-1,18208
14	1,4	0,5	0,66	0,01412	-1,77312	17	1,4	0,33333	0,66	0,01412	-2,36416
15	1,4	0,5	1	0,0214	-2,68654	18	1,4	0,33333	1	0,0214	-3,58206
22	2,2	0,5	0,33	0,00706	-0,56417	25	2,2	0,33333	0,33	0,00706	-0,75223
23	2,2	0,5	0,66	0,01412	-1,12835	26	2,2	0,33333	0,66	0,01412	-1,50446
24	2,2	0,5	1	0,0214	-1,70962	27	2,2	0,33333	1	0,0214	-2,27949

Calculations for the sensitivity analysis, Diamter, length and velocitiy

Case	f	L	vds	dP
1	0,1	50	0,0635	1,15582
2	0,1	50	0,1143	0,64212
3	0,1	50	0,1397	0,52537
10	0,125	50	0,0635	1,44477
11	0,125	50	0,1143	0,80265
12	0,125	50	0,1397	0,65672
19	0,15	50	0,0635	1,73373
20	0,15	50	0,1143	0,96318
21	0,15	50	0,1397	0,78806
4	0,1	75	0,0635	1,73373
5	0,1	75	0,1143	0,96318
6	0,1	75	0,1397	0,78806
13	0,125	75	0,0635	2,16716
14	0,125	75	0,1143	1,20398
15	0,125	75	0,1397	0,98507
22	0,15	75	0,0635	2,60059
23	0,15	75	0,1143	1,44477
24	0,15	75	0,1397	1,18209
7	0,1	100	0,0635	2,31164
8	0,1	100	0,1143	1,28424
9	0,1	100	0,1397	1,05074
16	0,125	100	0,0635	2,88955
17	0,125	100	0,1143	1,6053
18	0,125	100	0,1397	1,31343
25	0,15	100	0,0635	3,46746
26	0,15	100	0,1143	1,92636
27	0,15	100	0,1397	1,57612

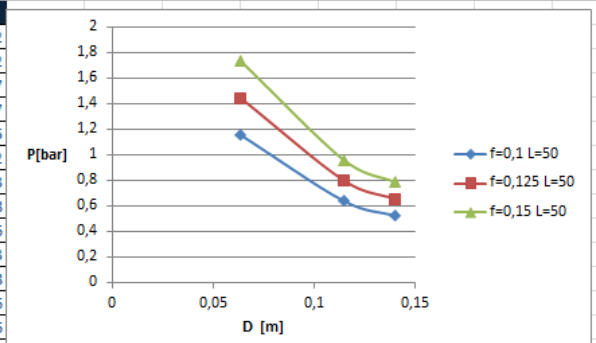

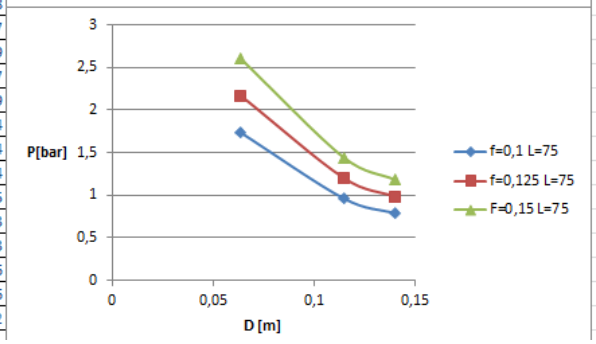

Case	f	L	vds	dP
1	0,1	50	1	0,525372
2	0,1	50	2	1,182087
3	0,1	50	3	2,101489
10	0,125	50	1	0,656715
11	0,125	50	2	1,477609
12	0,125	50	3	2,626861
19	0,15	50	1	0,788058
20	0,15	50	2	1,773131
21	0,15	50	3	3,152233
Case	f	L	vds	dP
4	0,1	75	1	0,788058
5	0,1	75	2	1,773131
6	0,1	75	3	3,152233
13	0,125	75	1	0,985073
14	0,125	75	2	2,216414
15	0,125	75	3	3,940291
22	0,15	75	1	1,182087
23	0,15	75	2	2,659697
24	0,15	75	3	4,72835
Case	f	L	vds	dP
7	0,1	100	1	1,050744
8	0,1	100	2	2,364175
9	0,1	100	3	4,202978
16	0,125	100	1	1,31343
17	0,125	100	2	2,955219
18	0,125	100	3	5,253722
25	0,15	100	1	1,576117
26	0,15	100	2	3,546262
27	0,15	100	3	6,304466

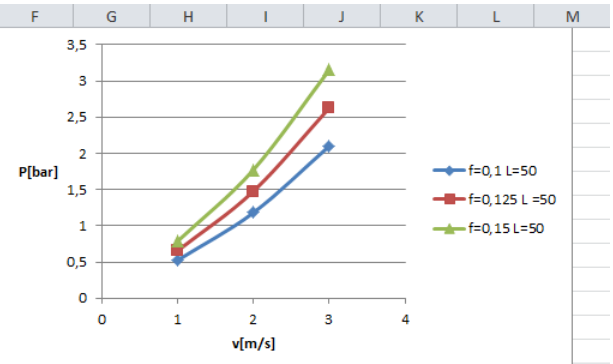

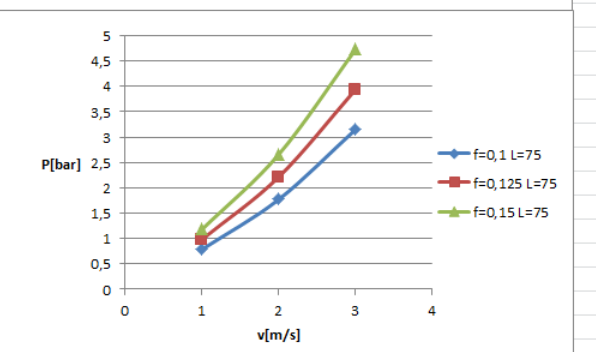

Case	f	L	vds	dP
1	0,1	50	1	0,525372
2	0,1	50	2	1,182087
3	0,1	50	3	2,101489
10	0,125	50	1	0,656715
11	0,125	50	2	1,477609
12	0,125	50	3	2,626861
19	0,15	50	1	0,788058
20	0,15	50	2	1,773131
21	0,15	50	3	3,152233
Case	f	L	vds	dP
4	0,1	75	1	0,788058
5	0,1	75	2	1,773131
6	0,1	75	3	3,152233
13	0,125	75	1	0,985073
14	0,125	75	2	2,216414
15	0,125	75	3	3,940291
22	0,15	75	1	1,182087
23	0,15	75	2	2,659697
24	0,15	75	3	4,72835
Case	f	L	vds	dP
7	0,1	100	1	1,050744
8	0,1	100	2	2,364175
9	0,1	100	3	4,202978
16	0,125	100	1	1,31343
17	0,125	100	2	2,955219
18	0,125	100	3	5,253722
25	0,15	100	1	1,576117
26	0,15	100	2	3,546262
27	0,15	100	3	6,304466

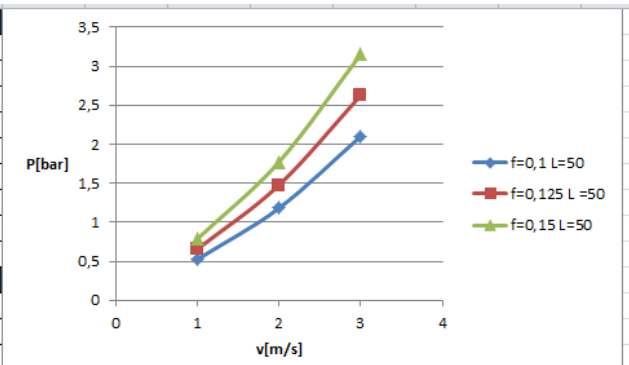

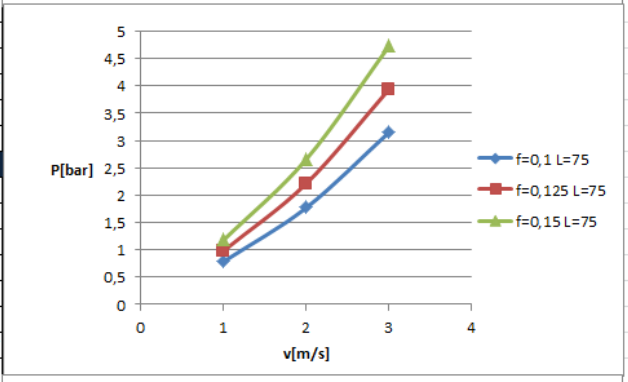

Appendix C

MATLAB script to calculate laminar flow conditions.

```
%MATLAB Program on 5 steps to cling and Surge And Swab
  %Use Paal Skalle's model from "Boreslam" kompedium

  %Decleration of various parameters

  rho=1200;              %kg/m3 – the density of the mud
  rho2=1350;             %kg/m3 – the density of new mud
  rhowater=1000;         %kg/m3 – the 75nside75 of sea water
  vds1=1.0;              %m/s – velocity of drill string while tripping
  vds2=1.5;              %m/s
  vds3=2.0;              %m/s
  vmud=5;                %m/s – velocity of drilling fluid
  R=0.108;               %m – Radius of well
  Rds=0.07;              %meter – radius of drill string
  Rc=0.01;               %Radius of drill string +cling
  R0=0.09;               %Radius to max velocity
  Pi=0;                  %mPa – The 75nside pressure of drill pipe
  Pann=0;                %mPa – The pressure in the annulus
  Pform=250*10^5;        %mPa – The pressure of the formation
  TVD=2000;              %Total Vertical Depth
  dwater=[1:200];        %meter – Depth of sea water
  g=9.81;                %m/s^2 – Gravitation
  tau=0;                 %Forces ( need to be looked at )
  DeltaP=0;              %mPa
  DeltaL=70;             %meter – Length of Bottom hole assembley
  qtot=100;              %m^3/s Total Bulk flow
  qpump=0;               %m^3/s Total pump flow
  qDS=0;                 %m^3/s Flow in Drill String
  K=0.20;                % Need numbers
  n=1;                   % n goes from 1 to 0,333
  n2=0,5 ;
```

```
  n3=0,333;
  Re=0;          %Reynolds number
  D=0.216;     % Diameter of wellbore
  my=0.15;        %Viscosity

%Area for the different sections [m^2]

  Across=pi*R^2;         % Well area
  Ashear=pi*R0^2;        % Max flow area
  Ads=pi*Rds^2;          % Drill String area
  Adsandcling=pi*Rc^2;    % Area of drillstring with clinged on mud
  Acling=Adsandcling-Ads; % Area of clinged area

%Forces involved in Surge&Swab

  tau= (DeltaP/(2*DeltaL))*(R-R0);

%Pressures:

%Bottom Hole Pressure:
Pbha=g*TVD*rho;

%Equation for the total flow, qtot

%Making the equation easier to handle by pulling constants together

%C1=pi^2*R^2;

%C2=((K*DeltaP)/(2*DeltaL))*((1/((1/n)+1))*(R-Rds));

%qtot=C1*(vds1*C2*(R^2-Rds^2));

%Finding DeltaP by rewriting the equation above.

        C1=pi^2*R^2;
```

```
        C2=K*(1/((1/n)+1))*(R-Rds)*(R^2-Rds^2);
disp('The change in pressure in wellbore is [mPa]')
   DeltaP=(((qtot*2*DeltaL)/(C1*C2))-(2*DeltaL*vds1)/((C2)))

disp('The pressure change in bar is:')
   DeltaP=(((qtot*2*DeltaL)/(C1*C2))-(2*DeltaL*vds1)/((C2)))/10^5

disp('The pressure in the Bottom hole assembley is [mPa]:')
   Pbha
disp('The pressure change in bar is:')
   Pbha/10^5

disp('Total pressure in wellbore when including surge/swab pressure is [bar]:')

Ptotal=(Pbha+DeltaP);
Ptotal/10^5


%Compairing total wellbore pressure with formation pressure:

disp('The formation pressure is [bar]:')

Pform/10^5

disp('If the pressure in the formation is higher than the pressure in the wellbore we are safe:')

 if Pform>Ptotal
   disp('Total well pressure is below the formation pressure, so continue')
      else disp('The well pressure is higher that formation frac pressure, email goes to resp.')
 end
```

```
Re=rho*vmud*D/my;

   disp('The Reynoldsnumber is:')
   Re
if Re<1800
     disp('The flow is laminar')
else disp('The flow is turbulent')

end
```